THREE-DIMENSIONAL HYDRAULIC CONDUCTIVITY TENSOR DETERMINATION

IN AN UNCONSOLIDATED ALLUVIAL AQUIFER

by

Michael D. Fort

submitted in partial fulfillment of requirements

for the degree of

Master of Science in Hydrology

New Mexico Institute of Mining and Technology

Spring 1992

DEDICATION

To my fellow graduate students, the foot soldiers of research.

"...And so each venture
Is a new beginning, a raid on the inarticulate
With shabby equipment always deteriorating
In the general mess of imprecision of feeling,
Undisciplined squads of emotion. And what there is to conquer
Once or twice, or several times, by men whom one cannot hope
To emulate-but there is no competition--
There is only the fight to recover what has been lost
And found and lost again and again: and now,under conditions
That seem unpropitious. But perhaps neither gain nor loss
For us, there is only the trying. The rest is not our business."

--T. S. Eliot

ACKNOWLEDGEMENTS

I would like to thank my advisor, Chia Chen for his support and advice during my M.S. program. Work reported here is financially supported by USGS(14-08-001-G1744) and WRRI(1423640). I would also like to thank Earl Downes, the driller, for putting up with us; Walter Gage, for all his help; and all the numerous people who have helped with details of the project and listened to me rant.

TABLE OF CONTENTS

LIST OF FIGURES

LIST OF FIGURES

LIST OF FIGURES CONTINUED

LIST OF TABLES

INTRODUCTION

The demand for accurate models of groundwater flow and transport in actual aquifers is continually growing. Before an aquifer can be accurately evaluated or modelled, the characteristic properties of the aquifer must be determined, such as hydraulic conductivity. The objective of this work is to use a three-dimensional well hydraulics theory to estimate the anisotropic hydraulic conductivities in an unconfined aquifer located at the Sevilleta Wildlife Refuge in New Mexico.

Hydraulic conductivity is the characteristic proportionality constant K that relates the flux to the gradient in Darcy's equation

$$q=-K\frac{dh}{dx} \qquad (1)$$

where q is the hydraulic flux, K is the hydraulic conductivity, and $\frac{dh}{dx}$ is the hydraulic gradient.

If the hydraulic conductivity is independent of the direction of groundwater motion, the aquifer is said to be isotropic, and the conductivity is a scaler. If the hydraulic conductivity does depend on the direction of groundwater motion the aquifer is said to be anisotropic under which conditions the conductivity is a second rank tensor. Anisotropy can result from the way in which sedimentary material is deposited. For example, laterally extensive, horizontal bedding will result in conductivities that are lower in the vertical direction than in the horizontal direction. In fluvial systems where channel deposits occur, the hydraulic conductivity along the channel will be higher than the hydraulic conductivity across the channel.

Regularly oriented fractures in consolidated rock can also result in anisotropic conditions.

In the most general case, anisotropic hydraulic conductivity is described by the second rank symmetric hydraulic conductivity tensor **K**, as

$$\boldsymbol{K}=\begin{bmatrix} K_{11} & K_{12} & K_{13} \\ K_{12} & K_{22} & K_{23} \\ K_{13} & K_{23} & K_{33} \end{bmatrix}$$

Due to its symmetry, the hydraulic conductivity tensor only has six unique elements. Using this most general case, Darcy's equation becomes

$$\begin{bmatrix} q_1 \\ q_2 \\ q_3 \end{bmatrix} = -\begin{bmatrix} K_{11} & K_{12} & K_{13} \\ K_{12} & K_{22} & K_{23} \\ K_{13} & K_{23} & K_{33} \end{bmatrix} \begin{bmatrix} \frac{\partial h}{\partial x_1} \\ \frac{\partial h}{\partial x_2} \\ \frac{\partial h}{\partial x_3} \end{bmatrix} \qquad (2)$$

where q_i is the hydraulic flux in the x_i direction and $\frac{\partial h}{\partial x_i}$ is the hydraulic gradient in the x_i direction.

The eigenvalues of the hydraulic conductivity tensor are known as the principal hydraulic conductivities, and the associated eigenvectors give the principal directions. Because the hydraulic conductivity tensor is symmetric, the principal directions will always be orthogonal, and the principal hydraulic conductivities will be real. If one or more of the coordinate axes is also a principal direction, the off diagonal terms associated with that axis will become zero. For example, if x_3 is a principal direction, then

$$\boldsymbol{K}=\begin{bmatrix} K_{11} & K_{12} & 0 \\ K_{12} & K_{22} & 0 \\ 0 & 0 & K_{33} \end{bmatrix}$$

It should be noted that in this case the hydraulic conductivity tensor only has four unique elements.

DETERMINATION OF HYDRAULIC CONDUCTIVITY

Typically, hydraulic conductivity is determined in the field by either withdrawing or injecting water from one well and observing the response in one or more monitor wells (i.e., the drawdown or pressure build up histories). In order to interpret the data from a well test, usually a well hydraulics analytical solution is used to analyze measured drawdown data.

In an aquifer that is homogeneous, isotropic, confined between two impermeable boundaries and of infinite extent and constant thickness; the drawdown in and observation well at a distance r from a fully penetrating well discharging at a constant rate is given by the well-known Theis solution. Due to it's simplicity and familiarity, the Theis solution is frequently used to evaluate well tests with conditions other than those stated above. If the aquifer does not meet the conditions described above the exclusive use of the solution can result in poor estimations of aquifer characteristics. Numerous other solutions have been developed for conditions not suited

to the Theis solution.

Hantush and Jacob (1955) developed a solution for aquifers that are homogeneous, isotropic, of infinite extent and constant thickness, but that are connected to a constant head source through a layer with lower hydraulic conductivity than the aquifer and no specific storage. Hantush (1960) extended this solution to allow for specific storage in the aquitard but retained the constant head source. Neuman and Witherspoon (1969) further extended this solution to allow for both specific storage in the aquitard and drawdown in the unpumped source.

Hantush (1964) presented solutions for partially penetrating wells in both confined and leaky aquifers. Because a partially penetrating well creates vertical and horizontal flow, Hantush (1964) also allowed for vertical hydraulic conductivity to be different from the horizontal. Weeks (1969) used the Hantush (1964) solution to develop a method for determining the vertical hydraulic conductivity, and the geometric average horizontal hydraulic conductivity using data from a partially penetrating pumping well and partially penetrating observation well.

Papadapoulos (1965) derived an equation for determining the horizontal anisotropy. The conditions for Papadopoulos (1965) solution are the same as for the Theis solution but requires three observation wells. Way and Mckee (1982) combined the Weeks (1969) and Papadopoulus' (1965) solutions to allow the determination of the full hydraulic conductivity tensor assuming that the vertical direction is a principal direction.

Hsieh and Neuman (1985) developed solutions for determining the full hydraulic conductivity tensor, without making any assumptions about principal directions. Solutions for four cases are given by Hseih and

Neuman (1985): a point source and point observation, a line source and a point observation, and point source and line observation, and line source and line observation. All four cases have been derived for an infinite medium, but no flow and constant head boundaries can be dealt with using image theory.

The application of Hsieh and Neuman's (1985) solution to field testing requires a partially penetrating pumping or injecting interval, and six partially penetrating observation intervals. In order to obtain the necessary three-dimensional flow conditions, the pumping/injecting interval and the observation intervals must be arranged in an appropriate three dimensional pattern. The observation intervals must also be sufficiently close to the pumping/injecting interval for three dimensional flow conditions to prevail. Typically, vertical flow will persist for a radial distance of one and one half times the aquifer thickness from the pumping/injecting interval.

All of the techniques developed for confined aquifers can be used for unconfined aquifers if it can be assumed that the water table is a fixed no flow boundary. If this assumption is made, then specific yield is substituted for storativity, and the initial location of the water table is used to determine aquifer thickness. These assumptions are generally valid at later times, if the drawdown is negligible. However, early time data frequently exhibits a specific yield that apparently increases with time. This apparent time dependence of specific yield is commonly known as delayed yield.

In order to overcome the apparent time dependence of specific yield in unconfined aquifers, Boulton (1955) proposed a delay mechanism in which specific yield is constant; but in which the water is not immediately

released from storage. The physical model that is the basis for Boultons (1955) solution places a thin layer of lower hydraulic conductivity at the top of the aquifer from which water drains into the aquifer. The rate at which the water drains from the lower hydraulic conductivity layer is determined by an empirical constant. Two of the major assumptions made in this solution are that there is negligible flow from the top layer into the well, and that the input from the top layer into the lower layer produces no vertical flow.

Streltsova (1972) examines the case of horizontal radial flow in an aquifer with input at the top due to the decline of the free surface. When a linearized finite difference boundary condition is applied to Streltsova's (1972) solution it takes the form of Boulton's (1955) solution. The linearized boundary condition presented by Streltsova (1972) gives physical meaning to Boulton's (1955) empirical constant by relating it to length of the vertical flow path from the upper boundary to the well. Streltsova (1972) estimates the length of the vertical flow path to be equal to one third of the total aquifer thickness.

Neuman (1972) developed a solution that includes the vertical head distribution; as opposed to Boulton's (1955) solution and Streltsova's (1972) solution which both use vertically averaged head. Neuman's (1972) solution also allows for the vertical hydraulic conductivity to differ from the horizontal hydraulic conductivity. Neuman (1975) extended his results to the case of partially penetrating wells, making this the most general solution for unconfined aquifers.

This paper is part of a study to evaluate the hydraulic conductivity at a field site located on the Sevilleta Wildlife Refuge, thirty miles north of Socorro, New Mexico. The results of this evaluation will be used in

modelling a later tracer study intended to examine the scale dependence of dispersion. The solution developed by Hsieh and Neuman (1985) was chosen as the principal method of evaluation because it required the least prior knowledge about the anisotropy at this location. In order to obtain the necessary data, a well field was designed and installed. In addition to the design requirements imposed by the chosen analytical method, and its intended use in the tracer test, the well field design was further constrained by budgetary considerations and available drilling equipment. This paper details the design and installation of the well field; as well as the results and analysis of preliminary pumping tests.

Specifically, the objectives of the current study are:

(1) Design piezometer nests suitable for depth specific water level measurements and depth specific water sampling.

(2) Develop the drilling technique required for the installation of the piezometers.

(3) Install the piezometers and test them to ensure that they function properly.

(4) Perform pumping tests while measuring water levels in the piezometers.

(5) Perform preliminary data analysis to estimate the hydraulic conductivity tensor.

EQUIPMENT DESIGN AND INSTALLATION

Because the hydraulic conductivity tensor is fully described by six independent quantities, a minimum of six observation points arranged in an appropriately three-dimensional pattern are required. Ideally, the hydraulic conductivity tensor could be determined from six observations; however, poor results may be obtained due to measurement error and local heterogeneities. In order to meet this requirement, six multilevel sampler/piezometers were installed surrounding a central pumping well (Figure 1).

DESIGN OF MULTILEVEL OBSERVATION WELLS

The purpose of the multilevel sampler/piezometer clusters is to allow depth-specific water samples and water levels to be taken at a single borehole. The traditional method of 'nesting' several boreholes completed at different depths is costly and can disturb the natural flow field. A multilevel sampler/piezometer installed in a single borehole reduces the amount of drilling required and hence the cost and disruption of the aquifer. In addition, the sampler/piezometers in a given borehole can be assumed to be located at a single point in the horizontal plane.

The key issues in designing multilevel sampler/piezometers are that the screened intervals must be hydraulically isolated from one another, and the screened interval must have good hydraulic connection with the aquifer. In a single partially penetrating piezometer the annulus around the screen is normally gravel packed to ensure good hydraulic contact with the aquifer

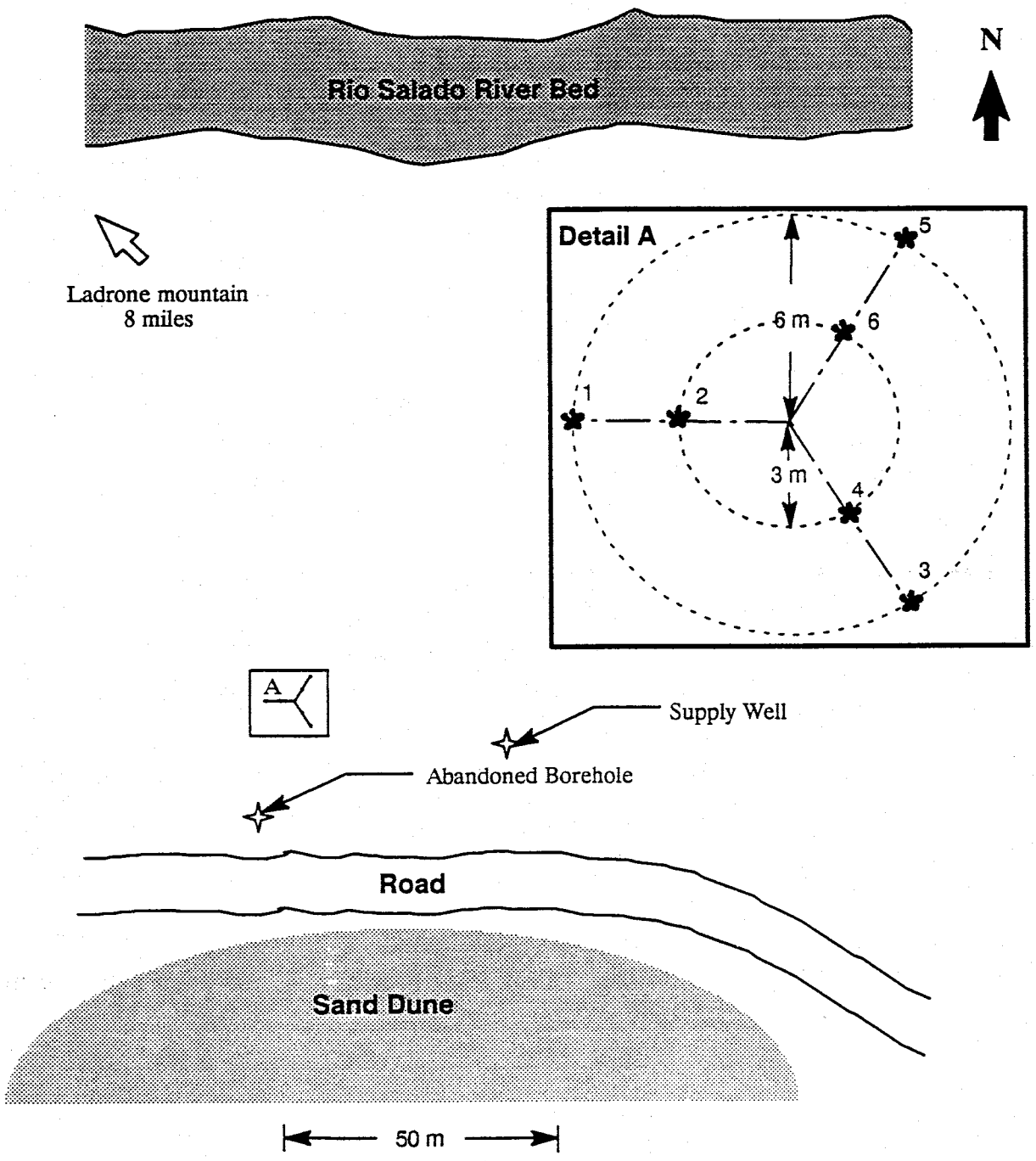

Figure 1: Layout of Well Field

and the annulus above the screen is filled with bentonite and/or grouted to ensure the screen is isolated from the rest of the aquifer. Because the screened intervals in these sampler/piezometer are so small and so closely spaced, it would be difficult to accurately place the gravel packs and a slight misalignment could be disastrous. For this reason, it was decided to backfill the annulus with drill cuttings in order to make the hydraulic conductivity in the annulus approximately the same as the aquifer hydraulic conductivity.

The original sampler/piezometer design was based on the use of 6 inch PVC casing to house the sampling tubes and piezometers. Before installing this casing, 3/4 inch I.D. ports (openings) are cut into the wall of the casing at various depths. On the inside of the casing these ports are connected to 3/8 inch I.D. tubing long enough to extend from the depth of the port to twenty feet below the surface. In the top twenty foot section of casing a 3/4 inch PVC pipe is installed for every port.

This sampler/piezometer cluster can be installed by first drilling a 7-3/8 inch borehole. The six inch casing is then installed in twenty foot sections. Before a new section is added to the string of casing already in the hole, all the tubes from the lower sections are threaded through it. When the top twenty foot section is reached, each tube is connected to a 3/4 inch I.D. PVC and the entire string is lowered into the borehole until the top of the casing is near the ground surface. The 3/4 inch PVC pipe allows water level measurements to be taken using a sounder or tape as long as the water levels are above twenty feet; which is the case, even during pumping, at this field site.

One sampler/piezometer of this design was fabricated but never

installed due to the change of drilling rig as discussed in the section on drilling history. To allow installation using a 3-1/4 inch I.D. hollow stem auger, the 6 inch casing had to be eliminated from the design. The new design, like the original, has 3/8 inch flexible tubing running from the measuring point to twenty feet below the surface where they are connected to rigid PVC pipes. In the new design, however, the tubes and pipes are not housed in a casing but tied together into a bundle. In order to allow more piezometers to be installed in a single borehole, the size of the upper standpipes was reduced from 3/4 inch PVC to 1/2 inch PVC. In addition to seven piezometers, eleven 1/8 inch I.D. tubes are to be used to obtain depth specific water samples (Figure 2).

This design is installed by drilling with a hollow stem auger. The bundled, flexible tubing with a weight attached to the end is lowered into the hollow portion of the auger. When the entire length, including the upper standpipe section, has been lowered into the augers, the augers are simply pulled out from around the bundle, leaving the bundle in place. In order to keep the bundle straight, a nylon rope, running the entire length of the bundle, is kept tight as the augers are pulled out.

Overall, this design is less expensive and easier to install than the original design. Its advantages are:

1. Six inch casings are not needed.
2. Field fabrication is not required.
3. The simpler auger drilling method can be used.
4. More sampling points can be obtained.

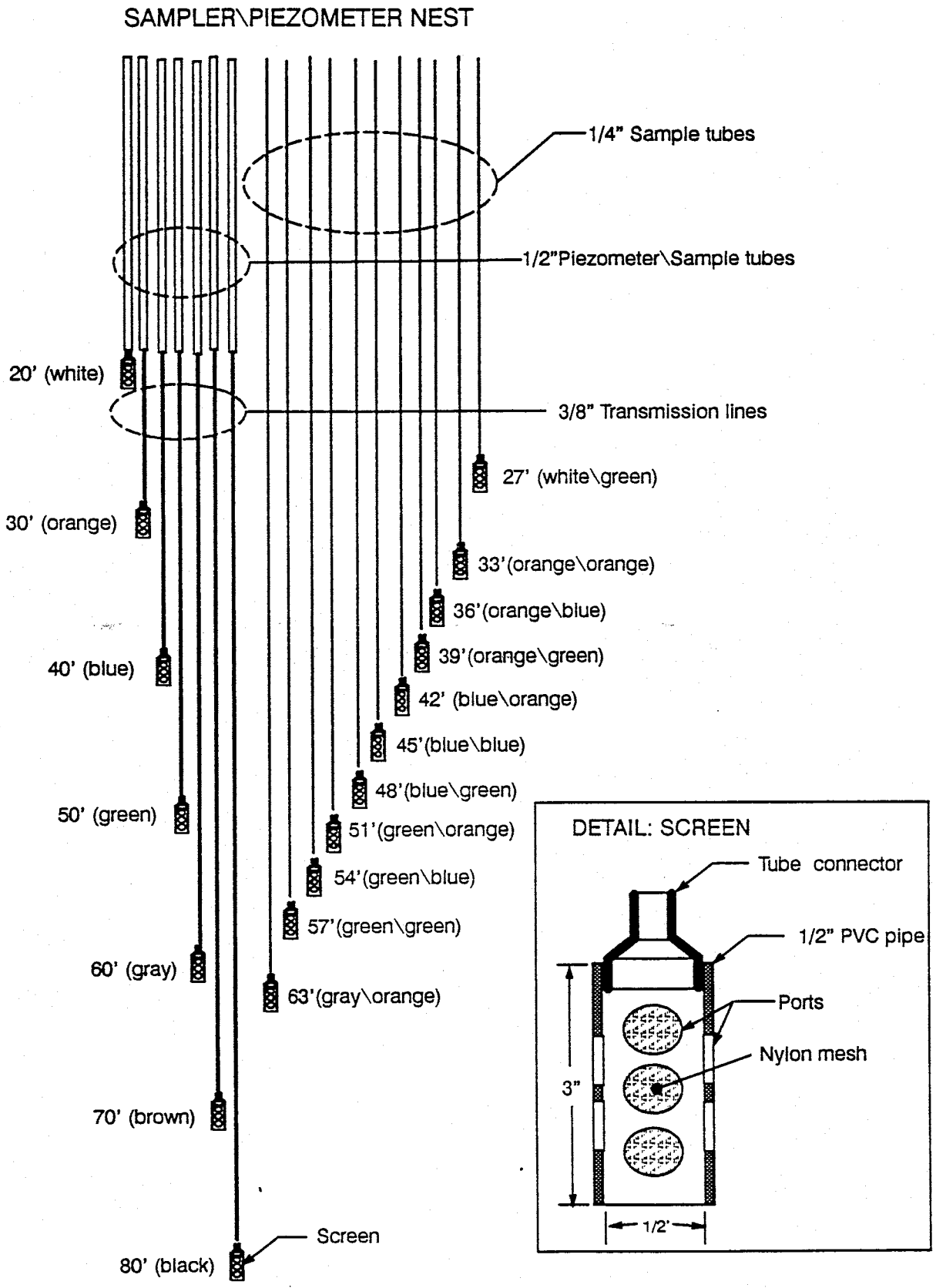

Figure 2: Multilevel Sampler/Piezometer Nest Construction

DRILLING HISTORY

The original design called for a six-inch center well surrounded by 9 multilevel samplers and 24 piezometers. Having recognized the difficulties in drilling in unconsolidated sandy materials, it was decided to reduce the number of boreholes by developing the multilevel observation well technique. Each of the multilevel observation wells can produce depth-specific drawdown data as well as depth-specific groundwater samples. This method eliminated the need for 24 boreholes for piezometers, while more than sufficient drawdown data for accomplishing the project can still be acquired. Drilling for the multilevel observation well began on 21 March 1990 using a 7-3/8 inch tricone rotary bit. In order to avoid the formation of wall cake, a synthetic polymer agent was used instead of drilling mud to remove the cuttings. The first borehole was completed to a depth of 85 feet and the screen was inserted to a depth of 40 feet where it was stopped by an obstruction possibly caused by caving at the lower portion of the borehole. After an unsuccessful attempt to free the screen by drilling below it with a 4 inch bit, we decided to use that well to supply water for project needs. A second borehole, 150 feet from the first, was drilled and completed to a depth of 85 feet. The high water velocities needed for air lift had, however, caused severe caving near the surface, and this borehole had to be abandoned.

To avoid caving caused by air lift of the rotary bit, it was decided to use a 3-1/4 inch hollow stem auger for drilling. The piezometers and samplers were installed through the hollow stem during drilling. To fit the diameter of the hollow stem, the 6 inch PVC casing (originally designed for the multilevel observation well) was not needed and therefore, was not used. Drilling with the hollow stem auger began on 22 May 1990. It had been hoped that using the hollow stem auger would also allow split spoon samples to be taken; however, sand rising up in the hollow stem caused the split spoon to sand lock in the auger, making sampling impossible. In future drilling operations it is planned to modify the drilling and sampling equipment to overcome this problem. Without the split spoon, drilling proceeded to 85 feet with grab samples being taken from the cuttings brought up by the auger. The samplers and piezometers were installed without incident, and the annulus was backfilled with cuttings.

Having wished to test the design of this multilevel observation well before the installation of others, it was decided to install the 6 inch pumping well next. Because of the requirement of the 6 inch casing, the use of the 7-3/8 inch rotary drilling rig available to us was unavoidable. In order to keep the borehole open long enough to install the screen while avoiding the wall cake problem, a synthetic polymer viscosifier was used in the drilling fluid. The borehole was drilled to 85 feet, screened with 6 inch solid PVC pipe from the surface to 20 feet. After completion, the well was pumped using

air lift to remove the drilling fluid and the annulus was backfilled with cuttings. The well was then left for three days to allow the breakdown of any remaining polymer and then developed using air surging and air lift pumping. A pumping test was conducted, but no drawdowns could be measured in those piezometers of the first multilevel observation well. This was due to the problem of the intake area of each piezometer being too small which lead to easy clogging. After making the intake area larger (as shown in Figure 2), five additional multilevel observation wells were installed using the 3-1/4 inch hollow stem auger between August 3 and August 19. The first observation well had to be abandoned.

DEVELOPMENT OF INSTALLED PIEZOMETERS

After installation, piezometers need to be developed in order to improve the hydraulic connection between the intakes and the aquifer. In general, during drilling, the hydraulic conductivity in the zone immediately adjacent to the borehole tends to be reduced due to the disturbance of the aquifer matrix. Development of piezometers repairs the damage by removing the finer particles and a high hydraulic conductivity.

The piezometers and samplers in this well field were and are being developed by alternately injecting water under pressure and pumping until there are no noticeable finds. During injection, the water under pressure expands the matrix which allows the fine particles to be removed during pumping. Figure 3 shows a manifold system that allows one or more piezometers in a well to be developed simultaneously.

A qualitative slug test is used to determine if a piezometer has been sufficiently developed. In this test the piezometers are filled with water and the rate at which the water level falls is observed. Due to the high hydraulic conductivity of the aquifer and the small bore size of the piezometers, the water level falls too quickly to allow a quantitative test. At present, many piezometers and samplers have been satisfactorily developed.

During the installation of observation wells 3, 4, and 5, the tops of the piezometers were covered to prevent debris from the augers from falling into them. During the installation of observation wells 2 and 6, the tops were left open and the piezometers were kept filled with water. The piezometers that were not filled with water require more development due

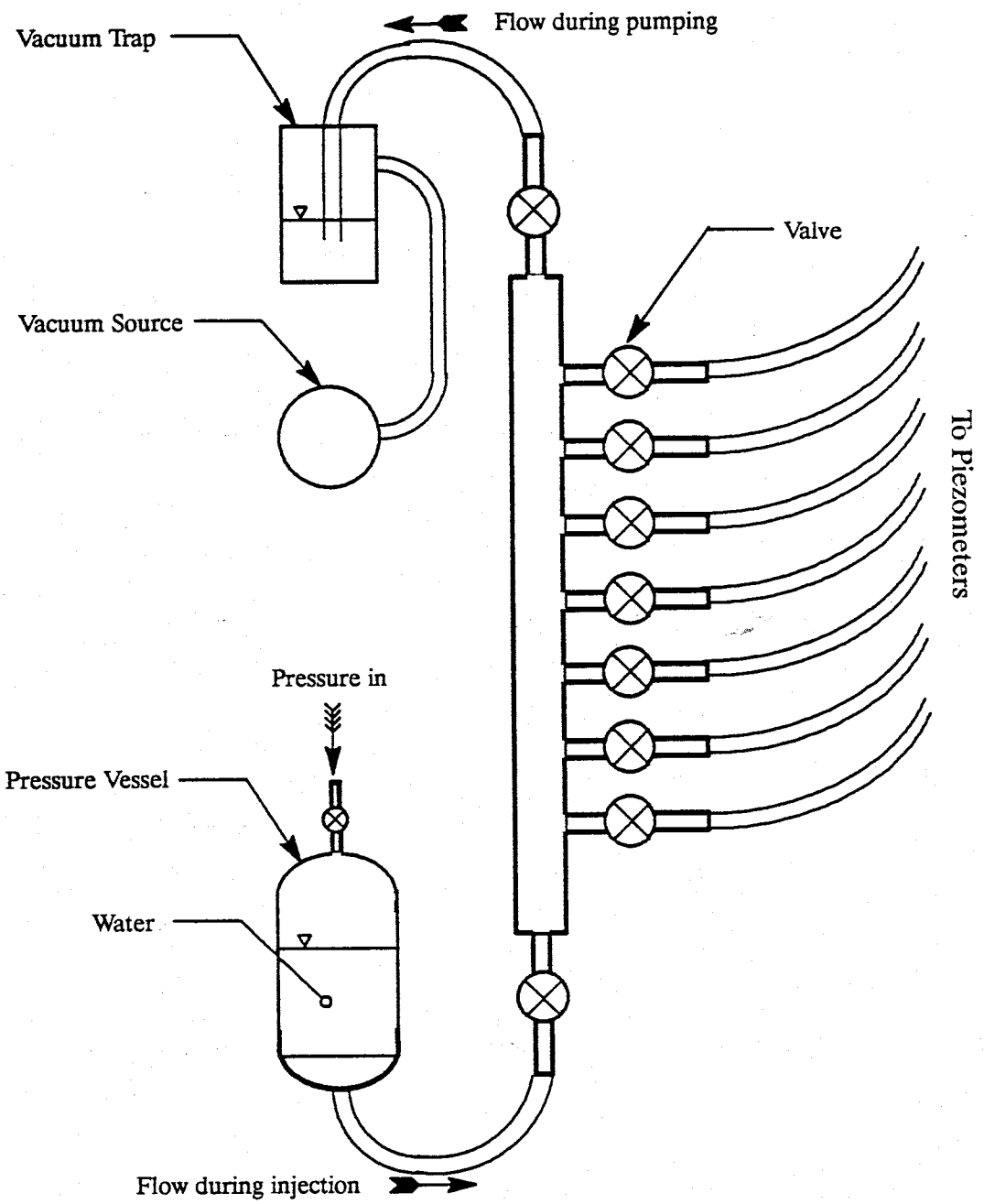

Figure 3: Schematic of Well Development Manifold

to clogging of the screens by fine sand and silt. The clogging results from water rushing in through the screen to fill the piezometer. This forces fine sand and silt from the soupy mix into the borehole and against the screen. This result should be noted during any future installation of piezometers.

A major concern on this project was the effect of backfilling the annulus around the piezometers with cuttings. The most likely result of this practice would be reduced hydraulic conductivity in the annulus due to the mixing of grain sizes. A less likely result would be a higher hydraulic conductivity due to filling with cuttings from a different, more conductive portion of the aquifer. A third possibility would be the formation of large unfilled voids around a piezometer screen, resulting in an effective screen length much longer than the actual screen length.

The most damaging of these three possibilities is the case of severely reduced hydraulic conductivity. Even a relatively thin layer of low hydraulic conductivity around the screen would significantly lower the transmissivity measured by that piezometer. The last two cases become significant problems only if they are so extensive that they cause too much interconnection between piezometers at different depths.

Pumping tests performed with the fully penetrating central well indicate that the piezometers were responding independently. The fully penetrating pumping test results also show that piezometers at the same depth but different locations respond similarly. If the annulus properties were having a significant effect, random responses at different locations would be expected. From the above results, it can be concluded with some confidence that the piezometers are measuring aquifer properties rather than those of the annulus.

GEOLOGY OF SEVILLETA FIELD SITE

The field site where the multilevel sampler/piezometers and pumping well are installed is located on the flood plain of the Rio Salado in the Sevilleta National Wildlife Refuge approximately 20 miles north of Socorro, New Mexico. In the region of the test site the Rio Salado is an ephemeral stream with the channel dry on the average of 320 days per year.

The aquifer in which the piezometers are installed consists of Holocene Rio Salado alluvium overlying Pleistocene axial stream deposits of the Sierra Ladrones Formation. The Rio Salado alluvium consists of interbedded sand, gravel, and silt. the axial stream deposits also consists of interbedded sand, and silt with occasional gravel and clay layers. Split spoon samples taken from three boreholes show the contact between the Rio Salado and axial stream deposits is located between 45 feet and 65 feet below the present ground surface. The increasing depth of contact from north to south indicates the original channel of the Rio Salado was located farther south than the present channel.

It was originally thought that the aquifer was confined to the Rio Salado alluvium (Zody, 1988). Later seismological studies (Knapp, 1991, personal communication) in the area and our own drilling indicate that the aquifer extends into the Sierra Ladrones formation. The total thickness of the aquifer is unknown, but it is assumed to be greater than 100 meters. Approximately 400 meters from the test site, the normal Loma Blanca fault cuts across the aquifer running almost due north-south. Zody (1988) found there was a marked steepening of the hydraulic gradient from the fault back for approximately 300 meters. It is unknown whether the effects of this fault

extend into the study area; however, there is little or no tilting of outcropping beds of the Sierra Ladrones formation in the vicinity of the test site.

DESCRIPTION OF PUMPING TESTS

At the present time, five partially penetrating pumping tests have been performed at the Sevilleta site. In order to create three-dimensional flow conditions, inflatable packers (Figure 4) were used to isolate 1.5 meters pumping intervals in the center well screen. The effectiveness of the packers had been previously tested by deflating the packers while continuing to pump. When the packers were deflated, the piezometers located well below the packed-off interval showed a rapid increase in drawdown, indicating the transition from partially penetrating to fully penetrating conditions.

During all five pumping tests, the outflow from the pump was measured using an orifice Weir. Table 1 gives a summary of the test conditions during each of the tests; refer to Figure 5 for definitions of the dimensions given.

In each of the five tests, the water levels were measured using electrical sounders. Due to the proximity of the observation wells to the pumping well, the drawdown in the observation wells approached steady state too quickly (less than about forty minutes) to allow sufficient transient data to be obtained for transient time analysis. Therefore, only steady state data will be considered in this paper. Figures 6 to 9 show the steady state drawdown at specific depths for Tests A, B, D, and E. No data was taken for Test C due to the low flow rate.

Table 1: Pumping Test Conditions.

TEST	Pumping Rate (m^3/s)	Depth to the Center of Pumped Interval (m)	Length of Pumped Interval (m)
A	3.20E-03	6.85	1.52 1.52
B	2.80E-03	16	1.52 1.52
C	NEGLIGIBLE	14.3	1.52 1.52
D	3.40E-03	17.22	1.52 1.52
E	3.59E-03	7.01	1.52 1.52

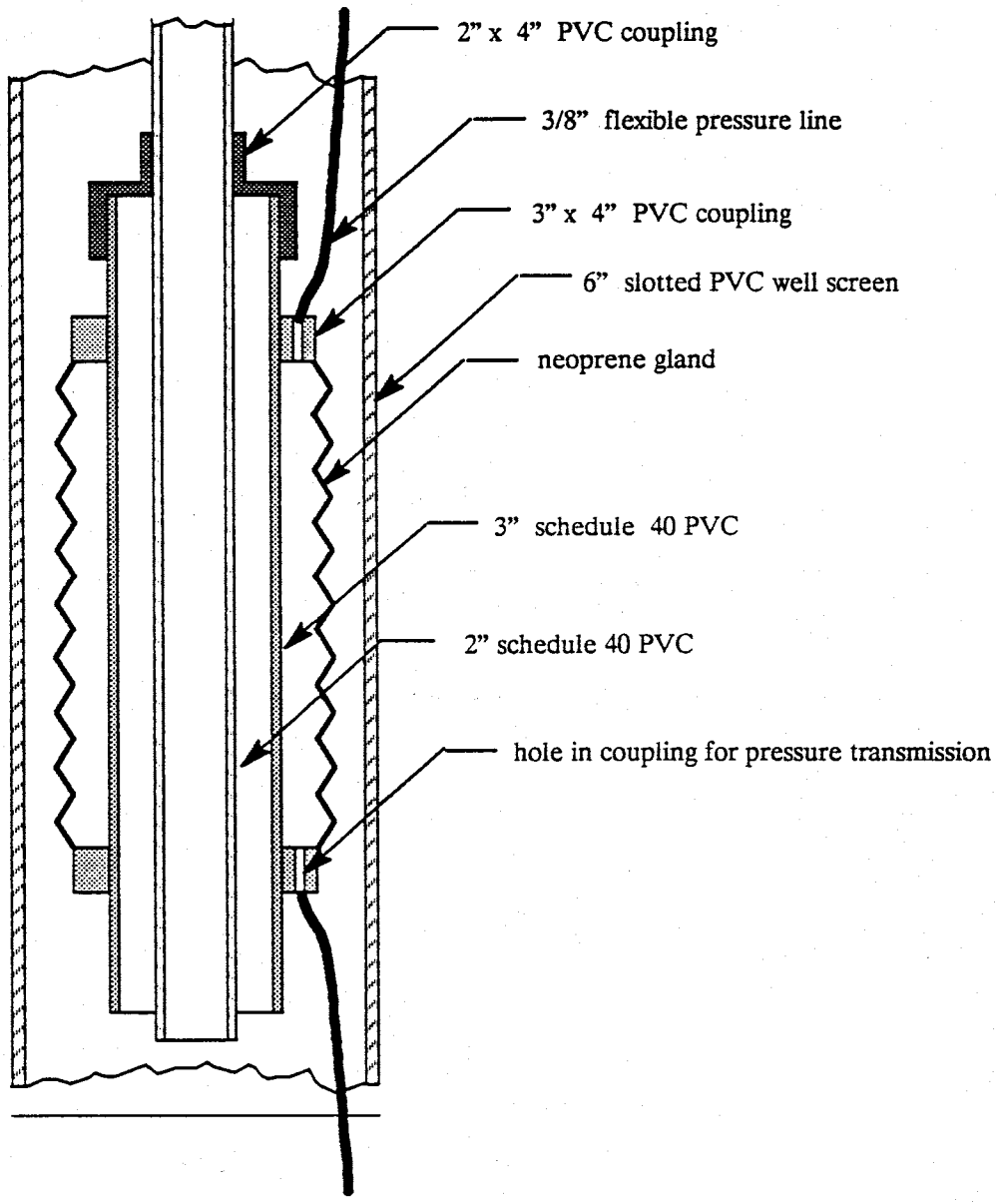

Figure 4: Schematic of Inflatable Packers

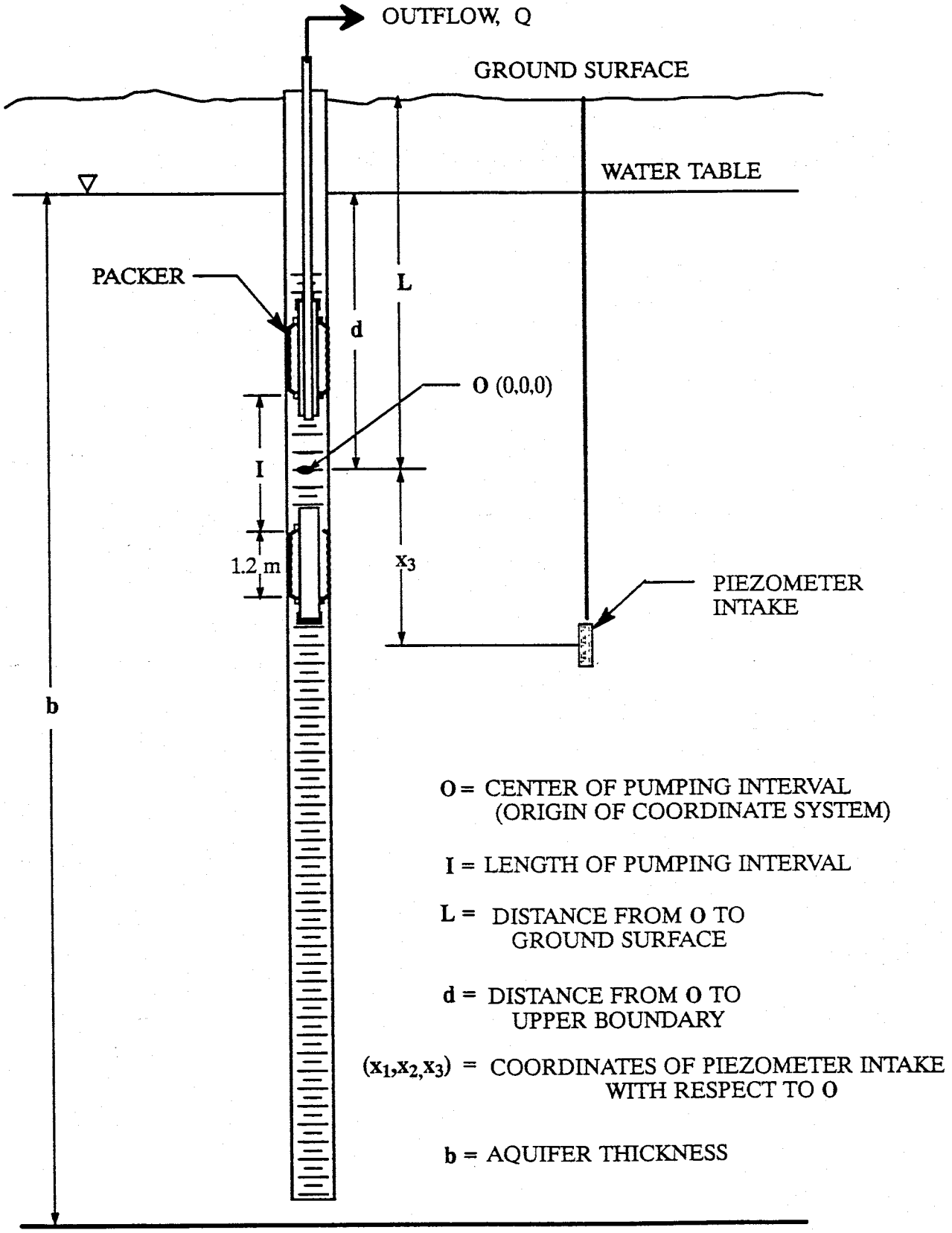

Figure 5: Layout for a Partially Penetrating Pumping Test

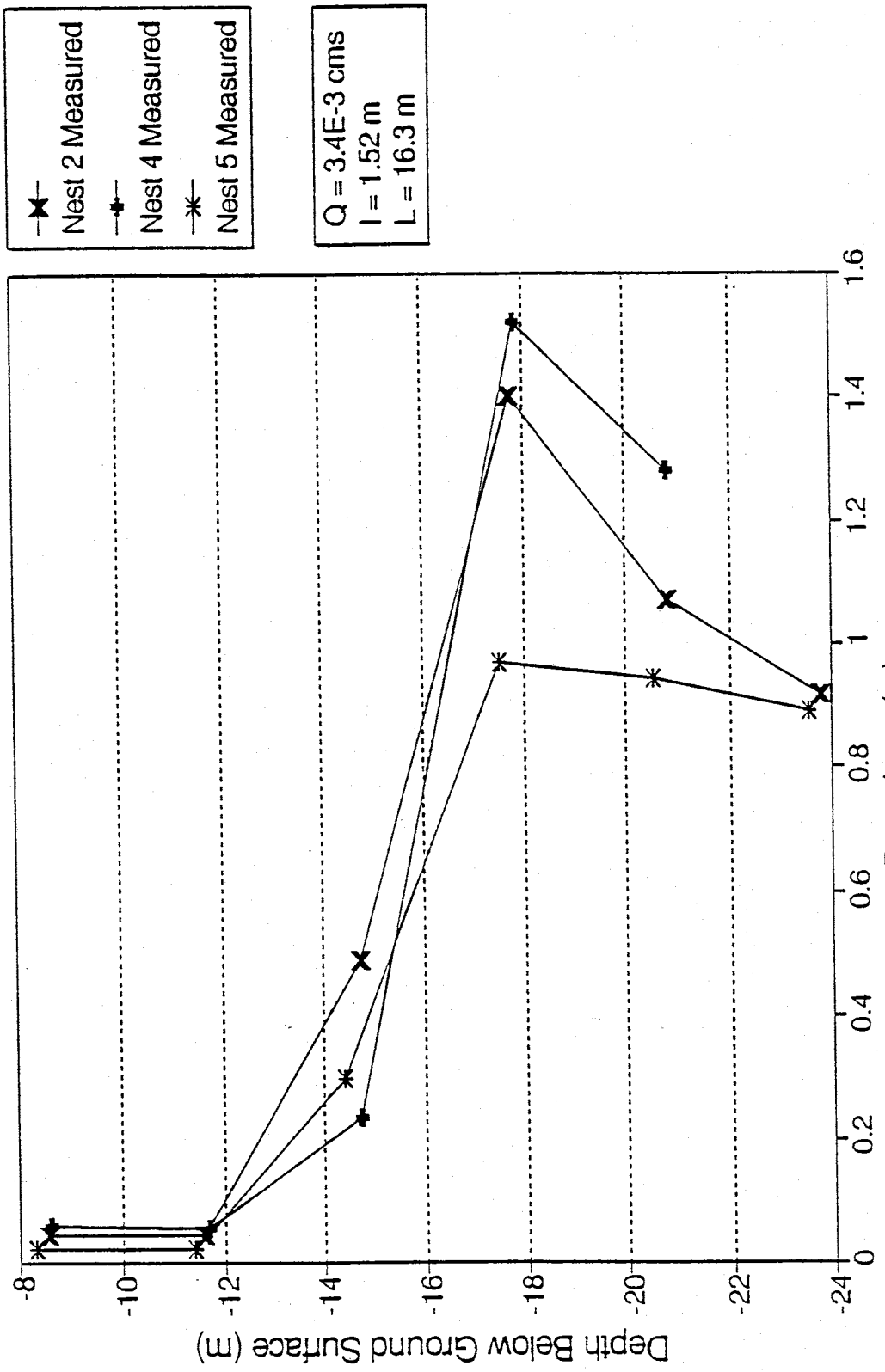

Figure 6: Measured Drawdown From Test D

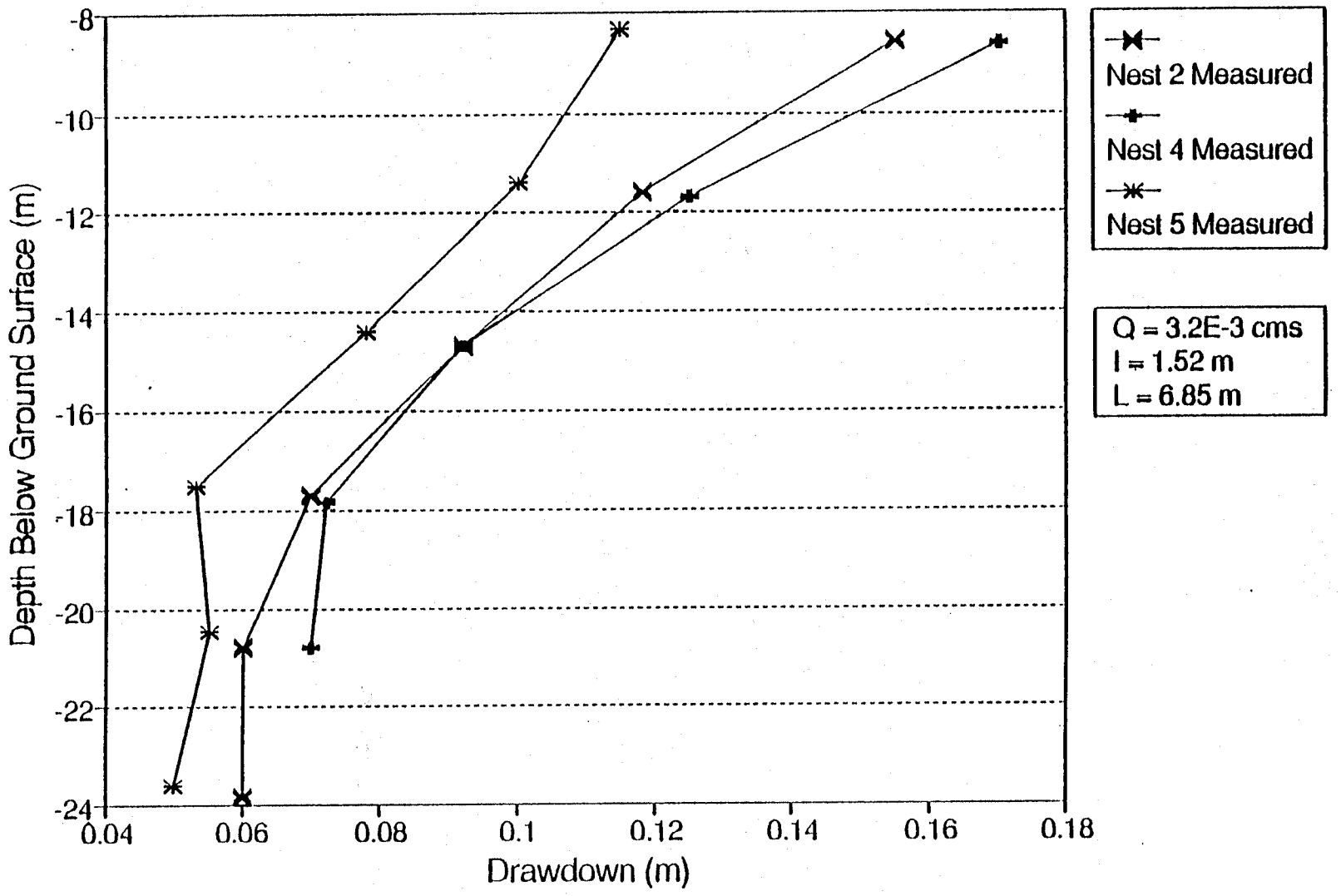

Figure 7: Measured Drawdown From Test A

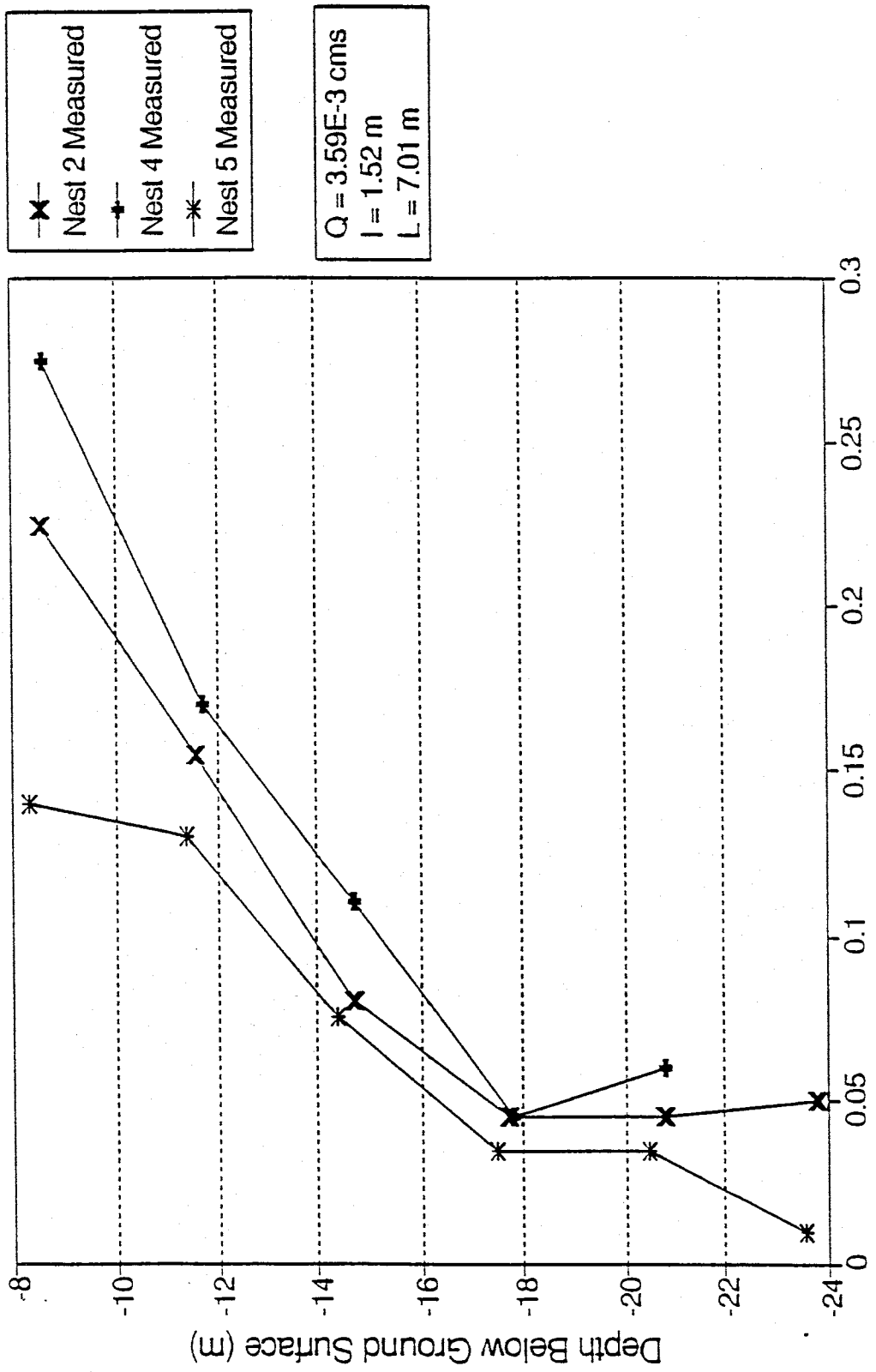

Figure 8: Measured Drawdown From Test E

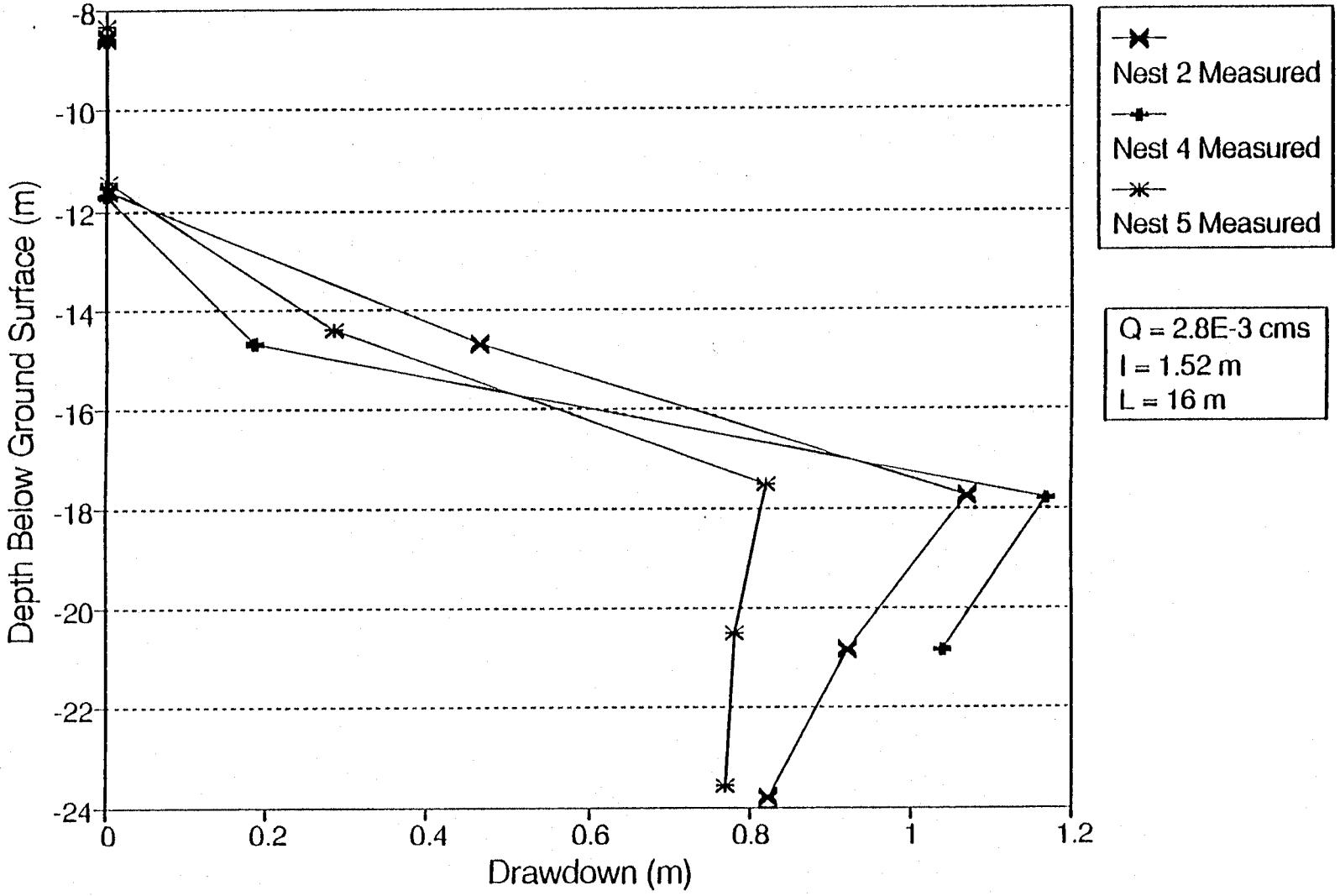

Figure 9: Measured Drawdown From Test B

QUALITATIVE ANALYSIS OF PUMPING TEST RESULTS

As stated in the section on the geology of the region, to the best of our knowledge, the aquifer extended continuously to a very large depth. The static water levels measured for Test A (Figure 7), and at previous times, showed the lowest water level at about fifteen meters and increasing both up and down. This distribution, however, indicated that some sort of heterogeneity existed at about 15 meters. Steady state drawdowns from tests using the full length of screen for pumping also show an anomaly at this depth.

Test B was performed with the center of the pumped interval at 16 meters to examine the effects of this possible heterogeneity. As shown in Figure 9, there was no measurable drawdown above 15 meters, showing that the suspected heterogeneity was in fact a low hydraulic conductivity layer.

In order to confirm the existence of this low hydraulic conductivity layer, the center of the packer was set at 14.3 meters for Test C. The intention was to have the pumped interval above the low hydraulic conductivity layer. The fact that the maximum obtainable flow rate was less than five gallons per minute, as opposed to 50 or 60 gallons per minute in Tests A and B, suggests that the pumped interval was in the low hydraulic conductivity layer, but still confirms it's existence. A notable difference between Tests A and B is that, in Test A, the maximum drawdown was less than one-fifth of the maximum drawdown in Test B; even though the pumping rates were almost the same. This shows that the lower layer is hydrologically distinct from the upper layer, and, overall, has a lower

hydraulic conductivity. Test D and E were performed in order to duplicate the results from Tests B and A respectively. The test conditions were slightly different from Tests B and A (Table 1), but the results were qualitatively the same. Figure 10 shows the aquifer geometry derived from this qualitative analysis.

The presence of drawdown in the lower piezometers in Tests A and E would seem to contradict the assumption of a low hydraulic conductivity layer. Those drawdowns, however, are probably the result of water flowing up through the screen and through the aquifer around the packer (Figure 11). This theory is supported by the fact that the drawdowns measured in the lower layer would produce virtually horizontal flow.

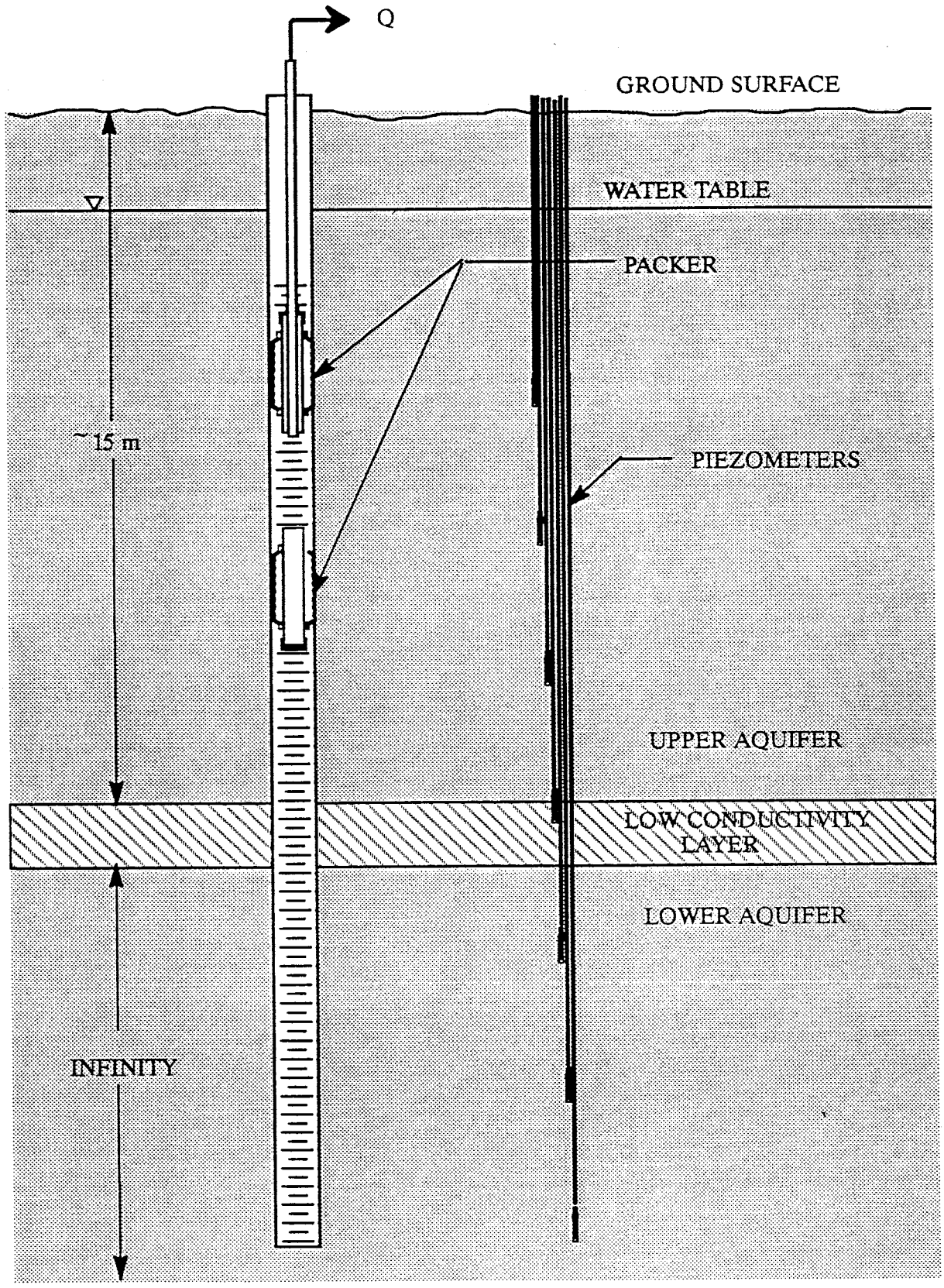

Figure 10: Two Layers and Low Conductivity Layer

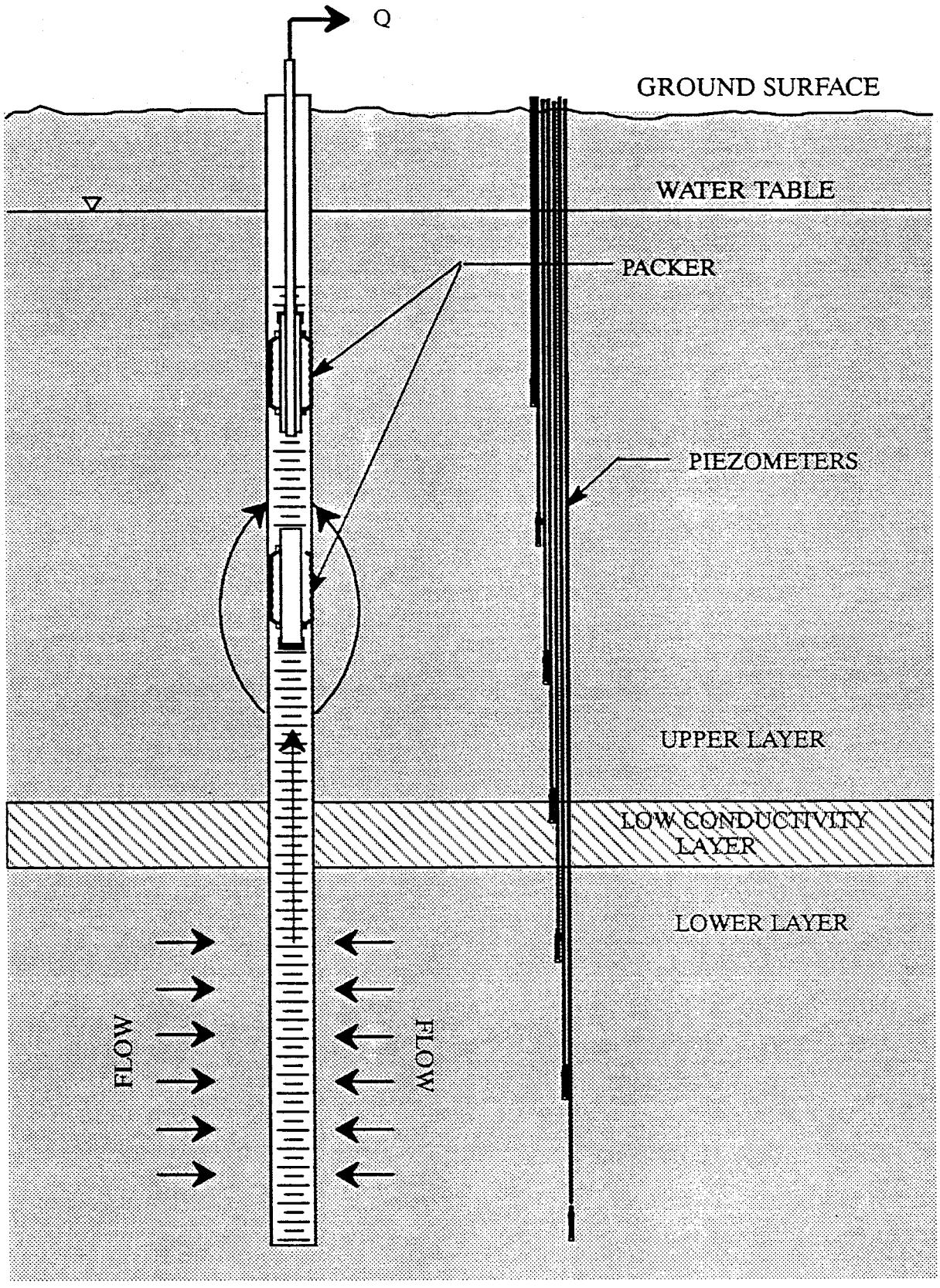

Figure 11: Flow Through the Low Conductivity Layer Via the Well Screen

QUANTITATIVE DATA ANALYSIS

Methodology:

From the qualitative analysis of the pumping test results, we have seen that there are two distinct layers separated by a low hydraulic conductivity layer. For the purpose of data analysis, this layer will be taken as an horizontal impermeable boundary. Because the drawdown is small compared to the aquifer thickness, the water table can also be taken as an horizontal impermeable boundary. Therefore, the upper layer will be analyzed as an aquifer of infinite lateral extent and 13 meters thick, bounded above and below by horizontal impermeable boundaries. The lower layer will be analyzed as an aquifer of infinite thickness and lateral extent bounded above by an horizontal impermeable boundary.

The purpose of this analysis is to determine the principal conductivities and their directions. The principal conductivities are the diagonal elements (K_{jj}) of a hydraulic conductivity tensor whose off diagonal terms (K_{ij} $i \neq j$) are equal to zero. The principal directions are the directions associated with each principal hydraulic conductivity and will be given by their compass bearing in the horizontal plane, and angle, above or below the horizontal plane. Because the principal directions are not known a priori, the following arbitrary working coordinates will be used for this analysis: $+x_1$ is east, $+x_2$ is west, and $+x_3$ is vertically up.

Although there are nine elements in the hydraulic conductivity tensor, due to symmetry only six are unique.In order to determine the full hydraulic

conductivity tensor in this coordinate system without making any assumptions about the principal directions; the technique developed by Hsieh and Neuman (1985) will be used.

DETERMINATION OF THE THREE-DIMENSIONAL HYDRAULIC CONDUCTIVITY TENSOR

The steady state drawdown at an observation point, due to a point sink in an infinite anisotropic aquifer, can be obtained from Equation (4) of Hsieh and Neuman (1985) by observing that the complimentary error function approaches unity as time approaches infinity. The result is

$$\Delta h = \frac{Q}{4\pi G_{xx}^{1/2}} \tag{3}$$

$$G_{xx} = \mathbf{x}^T \mathbf{A} \mathbf{x} \tag{3a}$$

where

$$\mathbf{A} = \begin{bmatrix} K_{22}K_{33} - K_{23}^2 & K_{13}K_{23} - K_{12}K_{33} & K_{12}K_{23} - K_{13}K_{22} \\ K_{12}K_{23} - K_{12}K_{33} & K_{11}K_{33} - K_{13}^2 & K_{12}K_{13} - K_{23}K_{11} \\ K_{12}K_{23} - K_{13}K_{22} & K_{12}K_{13} - K_{23}K_{11} & K_{11}K_{22} - K_{12}^2 \end{bmatrix}$$

the adjoint of **K**, Q is the volumetric pumping rate, **x** is the coordinates (x_1, x_2, x_3) of the observation point, with the point sink as the origin, and $\mathbf{x}^T$ is the transpose of **x**.

If, instead of an infinite aquifer, a planar boundary exists, the method of images can be used to mathematically remove the boundary. For the case of a single impermeable boundary, such as the lower portion of the aquifer being studied (Figure 10), the drawdown is

$$\Delta h = \frac{Q}{4\pi}\left(\frac{1}{G_{xx}^{1/2}} + \frac{1}{g_{xx}^{1/2}}\right) \tag{4}$$

$$g_{xx} = G_{xx} + 4Dd(d - \mathbf{m}^T\mathbf{x})/\mathbf{m}^T\mathbf{K}\mathbf{m} \tag{4a}$$

where

$$D = K_{11}K_{22}K_{33} + 2K_{12}K_{13}K_{23} - K_{12}^2K_{33} - K_{13}^2K_{22} - K_{23}^2K_{11}$$

the determinant of the hydraulic conductivity tensor **K**, d is the distance from the point sink to the boundary, m is the unit vector normal to the boundary, and $\mathbf{m}^T$ is the transpose of m.

If the planar boundary is normal to the x_3 axis (i.e. horizontal), then

$$\mathbf{m}^T\mathbf{x} = x_3 \tag{5}$$

and

$$\mathbf{m}^T\mathbf{K}\mathbf{m}=K_{33} \tag{6}$$

Substituting Equations (5) and (6) into Equation (4a) yields,

$$g_{xx}=G_{xx}+4Dd(d-X_3)/K_{33} \tag{7}$$

If both upper and lower impermeable boundaries exist, as in the upper portion of the aquifer being studied, an infinite number of image wells will be required to eliminate the boundaries.

In order to apply Equation (7), we must consider the distance d to an imaginary boundary associated with each image well. From image theory we know this boundary must lie halfway between the image well and the real well. Figure 12 shows the locations of the image wells and their associated imaginary boundaries. For the case shown in figure 12, the drawdown (Δh) at an observation point is calculated by

$$\Delta h=\frac{Q}{4\pi}\left(\frac{1}{G_{xx}^{1/2}}+\sum_{i=1}^{\infty}\frac{1}{(g'_{xx})_i^{1/2}}\right) \tag{8}$$

where

$$(g'_{xx})_i=G_{xx}+4Dd'_i(d'_i-x_3)/K_{33} \tag{9}$$

The ith value of d'is calculated by using the boundary for that image well in

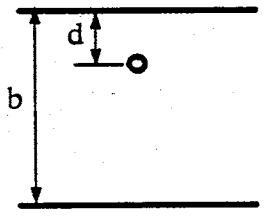

(A) Finite Thickness Aquifer

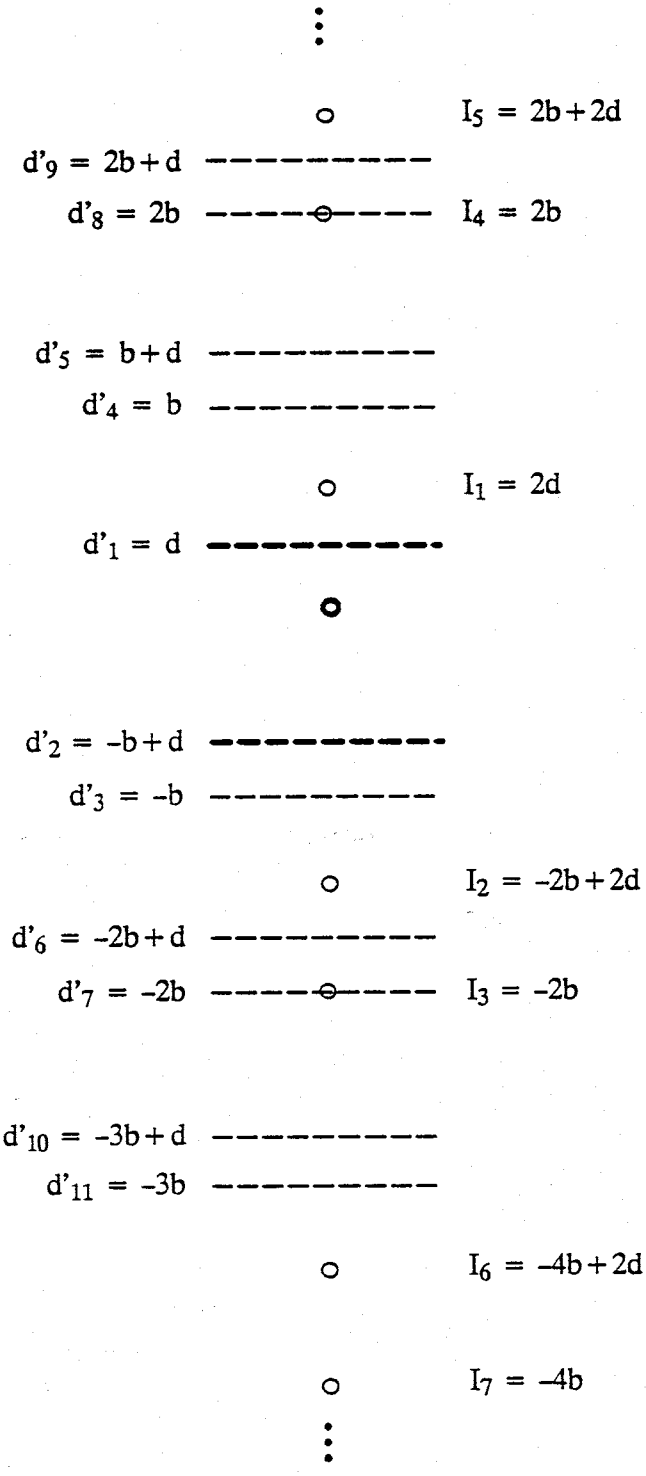

(B) Aquifer in (A) Expressed by Superposition Principal

- Real Point Sink
- Image Point Sink
- Real Boundary
- Imaginary Boundary
- d'_i = Distance from the Real Sink to the ith Imaginary Boundary
- I_i = Distance From the Real Sink to the ith Imaginary Sink

Figure 12: Linear Superposition of Representing (A) by (B)

Equation (7). The values of d' in terms of d are defined in Figure 12. Although the exact solution of Equation (8) requires an infinite number of image wells, the effect of each successive well decreases until it becomes insignificant, and further image wells can be truncated. This is analogous to ignoring real boundaries that are too distant to have significant influence on the results. In analyzing the data for this report, the image wells have been truncated when an additional four wells increase the drawdown at the observation point less than one-tenth of one percent. If the number of image wells is set equal to one then Equation (8) becomes identical to Equation (7).

The equations derived so far are for a point sink and a point observation. Even though in the actual pumping tests the pumped interval and observation interval have infinite lengths, they can be taken as points if (Hsieh and Neuman 1985)

$$(G_{xx}/G_{ll})^{1/2}>5 \tag{10}$$

and

$$(G_{xx}/G_{bb})^{1/2}>5 \tag{11}$$

where

$$G_{ll}=l^{T}\mathbf{A}l$$

$$G_{bb}=b_{T}\mathbf{A}l$$

l is the vector (l_1, l_2, l_3) representing the length and orientation of the pumped interval, and b is the vector (b_1, b_2, b_3) representing the length and orientation of the observation interval.

In all the pumping tests performed so far l=(0,0,1.52m) and b=(0,0,0.0076m). Because **A** is not known prior to the analysis the above criteria must be checked after the analysis. If any point fails to meet the criteria for a point sink or a point observation, then the analysis must be repeated omitting that point.

In order to determine the hydraulic conductivity tensor, a non-linear least squares algorithm is used to fit Equation (8) to pumping test data. The purpose of least squares fitting is to find the maximum likelihood estimate of model parameters by minimizing the merit function (X^2) which in this case is defined as

$$X^2=\sum_{i=1}^{N} [\Delta h_i-\Delta h(v_i;K')]^2 \qquad (12)$$

where Δh_i is the actual drawdown at point i, $\Delta h(v_i;K')$ is the drawdown calculated using equation 7, v_i represents the known variables (i.e., Q, $\mathbf{x}_i$, d_i, b_i, L), and K' represents the six unique conductivities to be identified, with

$K_1' = K_{11}$

$K_2' = K_{12}$

$K_3' = K_{13}$

$K_4' = K_{22}$

$K_5' = K_{23}$

$K_6' = K_{33}$

To minimize the merit function (Equation 12), an iterative approach is applied to the following set of six linear equations:

$$[\alpha_{kl}]\{\delta_l\} = \{\beta_l\} \quad l,k = 1,2,3,\cdots,6 \tag{13}$$

where $[\alpha]$ is a 6X6 square matrix, $\{\delta\}$ and $\{\beta\}$ are 6x1 matrices. In our case

$$\alpha_{kl} = 1/2 \frac{\partial_2 \chi}{\partial} K_k' \approx \sum_{i=1}^{N} \left[\frac{\partial \Delta h(\nu_i; \mathbf{K}')}{\partial K_k'} \cdot \frac{\partial \Delta h(\nu_i; \mathbf{K}')}{\partial K_l'} \right] \tag{14}$$

$$\beta_k = -1/2 \frac{\partial \chi_2}{\partial K_k'} = -2 \sum_{i=1}^{N} \left[\Delta h_i - \Delta h(\nu_i; \mathbf{K}') \right] \cdot \frac{\partial \Delta h(\nu_i; \mathbf{K}')}{\partial K_k'} \tag{15}$$

and δ_l is the correction to be added to K_1' .

Using equation (8) for Δh results in

$$\frac{\partial \Delta h(\nu_i; K')}{\partial K'_k} = -1/2 (G_{xx})_i^{-3/2} \frac{\partial (G_{xx})_i}{\partial K'_k}$$

$$-1/2 \sum_{i=1}^{\infty} [(g'_{xx})_i]^{-3/2} \cdot \frac{\partial (g'_{xx})_i}{\partial K'_k} \qquad (17)$$

and using equation (9) for g'_{xx} yields

$$\frac{\partial (g'_{xx})_i}{\partial K'_k} = 1/2 [(G_{xx})_i + \frac{4Dd'_i}{(} d'_i - x_3)]^{-3/2} \cdot [\frac{\partial (G_{xx})_i}{\partial K'_k} + (\frac{1}{K'_6} \frac{\partial D}{\partial K'_k} - D \frac{\partial (K'_6)^{-1}}{\partial K'_k})$$

$$\cdot 4d'_i (d'_i - x_3)] \qquad (18)$$

For example substituting K'_1 for K'_k in equations (16) and (17) yields

$$\frac{\partial (G_{xx})_i}{\partial K'_1} = (x_2)_i^2 K'_6 + (x_3)_i^2 K'_4 - 2 (X_2)_i (x_3)_i K_5 \qquad (18)$$

and

$$\frac{\partial (g_{xx})_i}{\partial K'_1} = 1/2 [(G_{xx})_i + \frac{4Dd'_i}{K'_6} (d'_i - x_3)]^{-3/2}$$

$$\cdot [\frac{\partial (G_{xx})_i}{\partial K'_1} + \frac{1}{K'_6} (K'_4 K'_6 - K'^2_5) \cdot 4d'_i (d'_i - x_3)] \qquad (19)$$

This set of six equations with six unknowns is solved for $\delta_1 \ldots \delta_6$; which are added to the previous values of $K_1 \ldots K_6$. The process is

then repeated, using new values for $K_1 \ldots K_6$ each time, until a minimum is reached. The process should be terminated when there is a negligible change in the merit function.

The above method works well when the initial guesses for hydraulic conductivity are close to correct. When the initial guesses are far from the correct values, convergence can be ensured by forcing the matrix to be diagonally dominant.

In the Levenburg-Marquardt method, this is done by letting

$$\alpha'_{ll} = \alpha_{ll}(1+\lambda) \tag{20}$$

and substituting α' for α in Equation (13) giving

$$[\alpha'_{kl}]\{\delta_l\} = \{\beta_l\} \tag{21}$$

Initially λ is chosen as some small value (for example, .01). If the merit function fails to decrease on a given iteration, λ is increased until the merit function does decrease. On each iteration that the merit function does decrease λ is also decreased. This means that as the values for hydraulic conductivity approach the correct values, Equation (21) approaches Equation (13).

RESULTS OF DATA ANALYSIS

The data from Pumping Tests A, B, D, and E were analyzed based on the assumption of two distinct layers separated by an impermeable boundary. The data from Tests A and E were used to analyze the upper layer assuming both upper and lower impermeable boundaries, and using Equation (18) in the least squares fitting program with 201 image wells. The lower layer was analyzed assuming only an upper boundary and using data from Tests B and D and Equation (18) in the least squares fitting program with one image well. In addition to analyzing each test separately, the data from Test A and E were analyzed simultaneously. The results of these analyses are shown in figures 13 to 19.

All of the points used met the criterion for being taken as a point sink and a point source. The data from the piezometers at 6 meters depth were not used due to their proximity to the water table and the resulting possible violation of the horizontal boundary assumption. The results of all six analyses are presented in Table 2.

Figures 20 to 27 show graphical representations of the hydraulic conductivity ellipsoids derived from Table 2. The ellipsoids are represented by three orthogonal, planar ellipses with their axes oriented along the principal directions. The length of each axis is equal to the square root of the hydraulic conductivity in that direction. Figures 20 to 22 represent the

ellipsoids for the upper aquifer and figures 23 to 25 show the ellipsoids for the lower layer at the same scale as figures 20 to 22. Closer views of the lower layer ellipsoids are shown in figures 26 and 27.

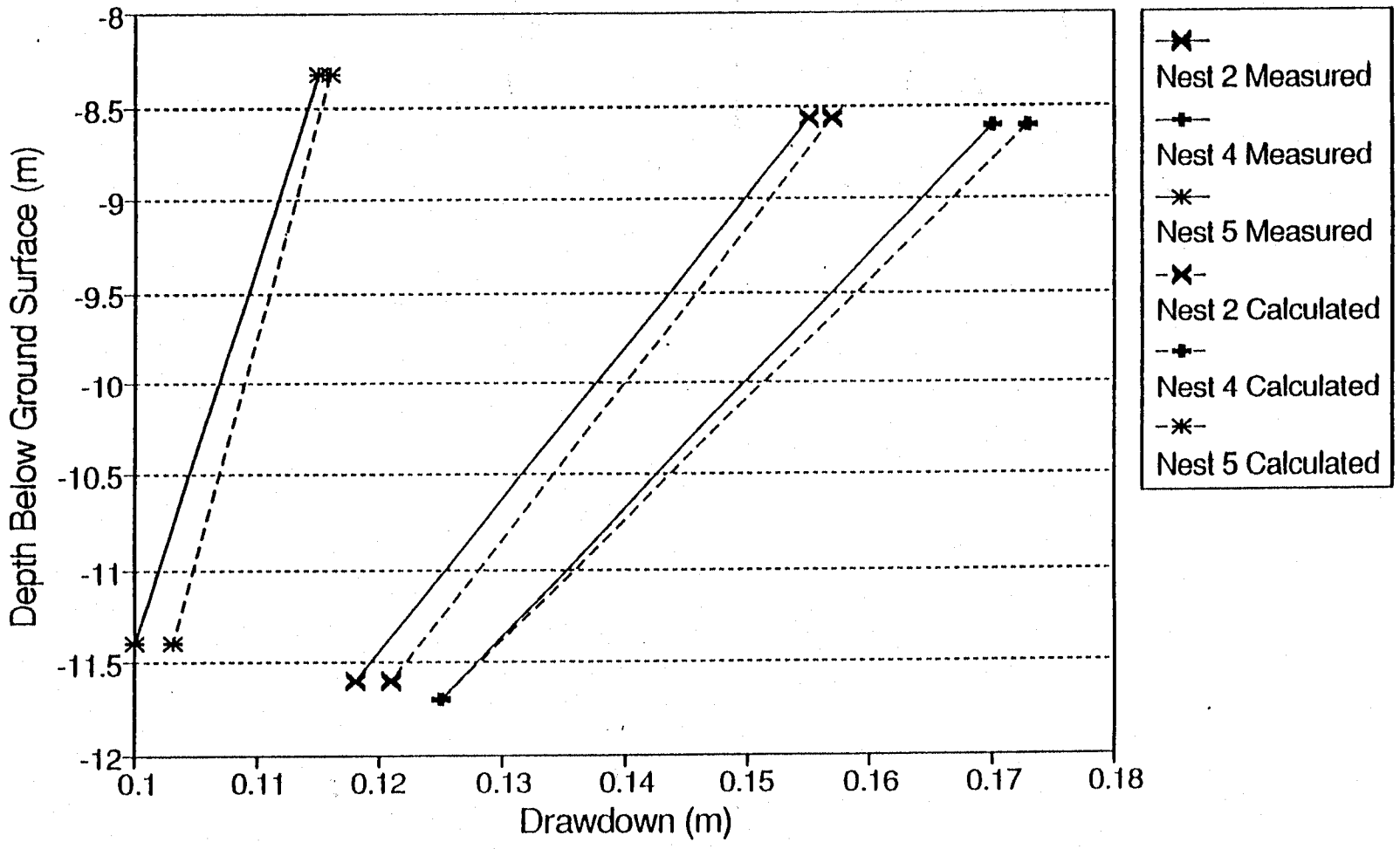

Figure 13: Measured and Calculated Drawdown for the Upper Portion of Test A calculated Drawdown is based on Fitting to Test A Data

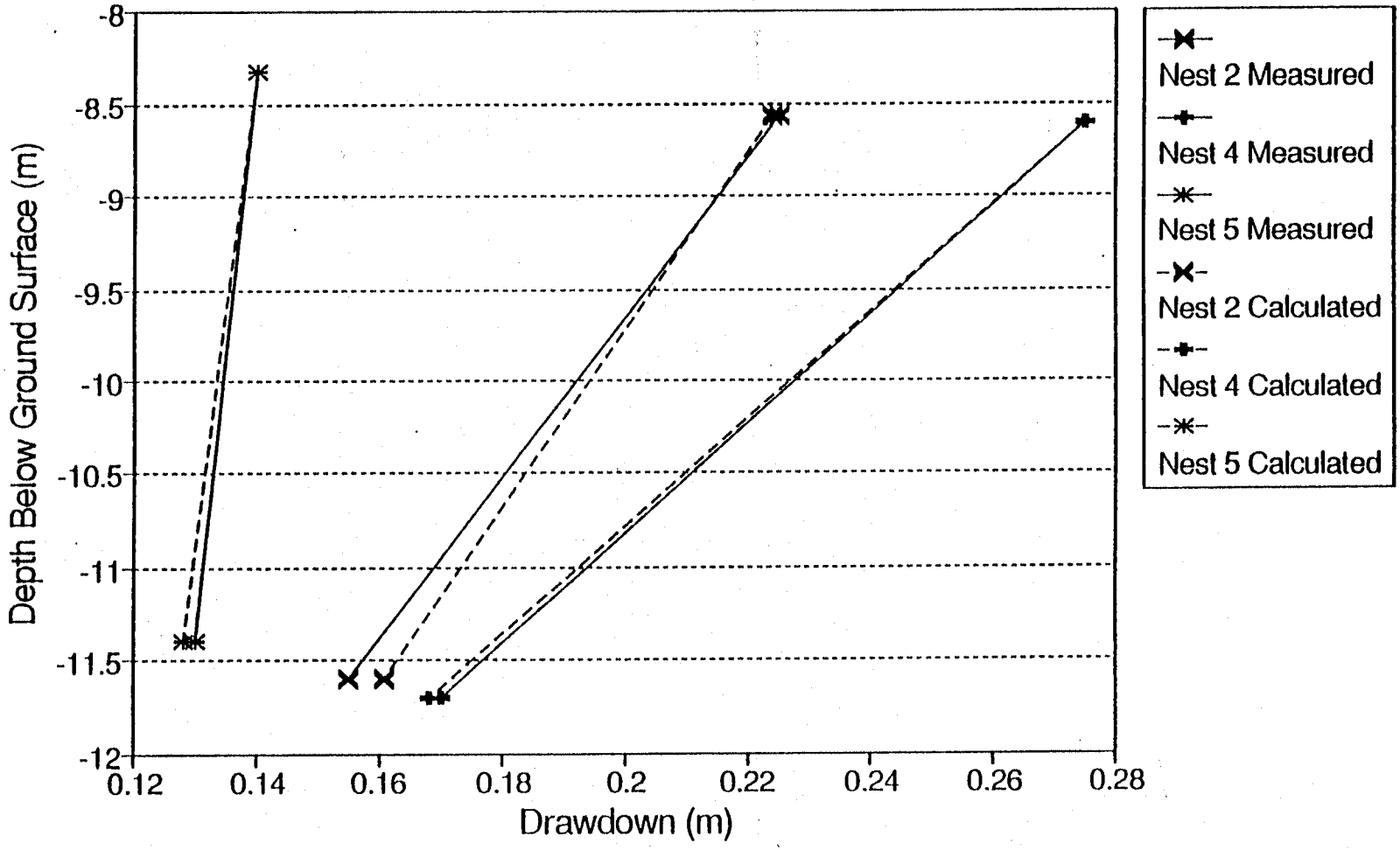

Figure 14: Measured and Calculated Drawdown for the Upper Portion of Test E. Calculated Drawdown is Based on Fitting to Test E Data.

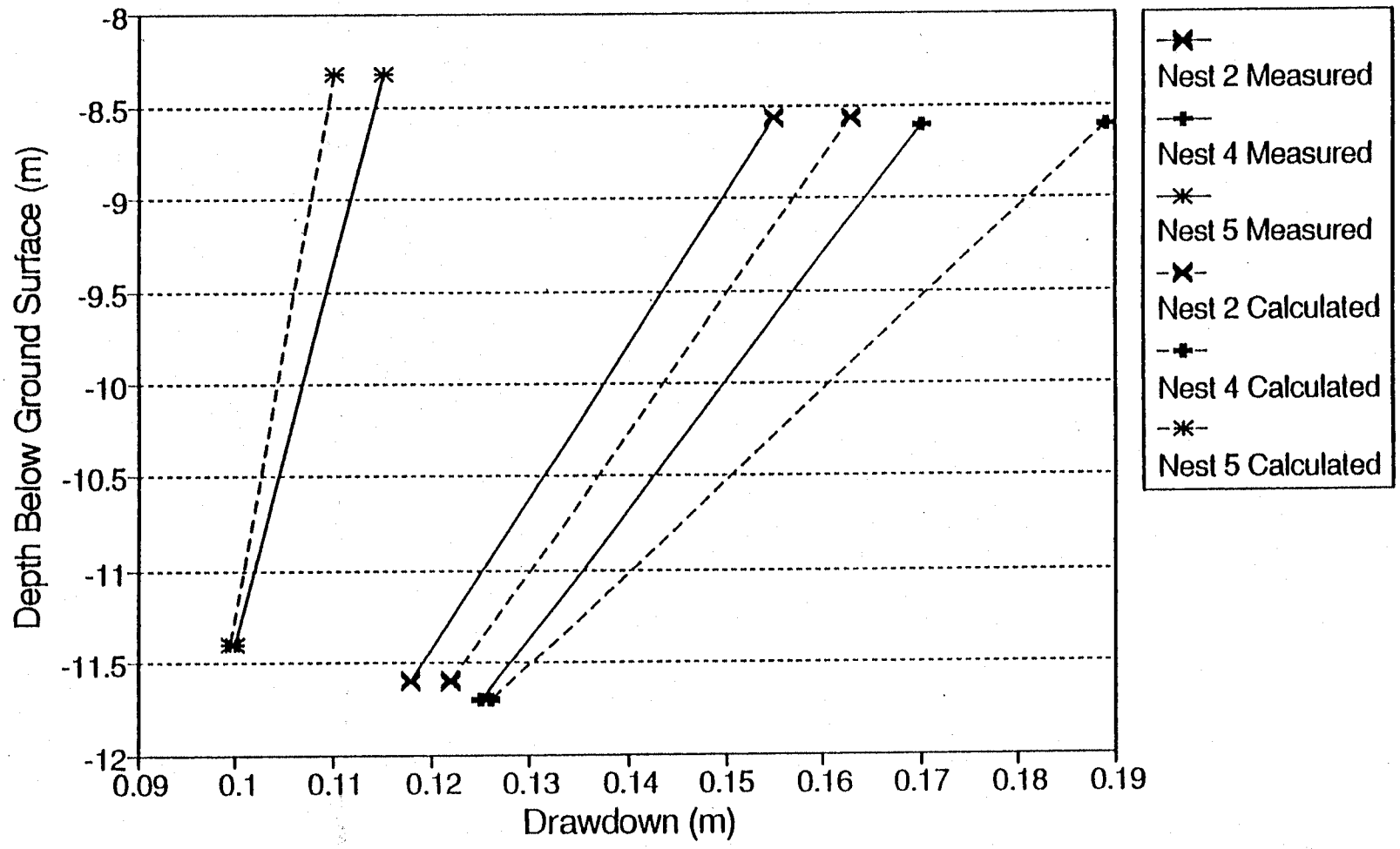

Figure 15: Measured and Calculated Drawdown for the Upper Portion of Test A Calculated Drawdown is based on Fitting to Test A and Test E Data

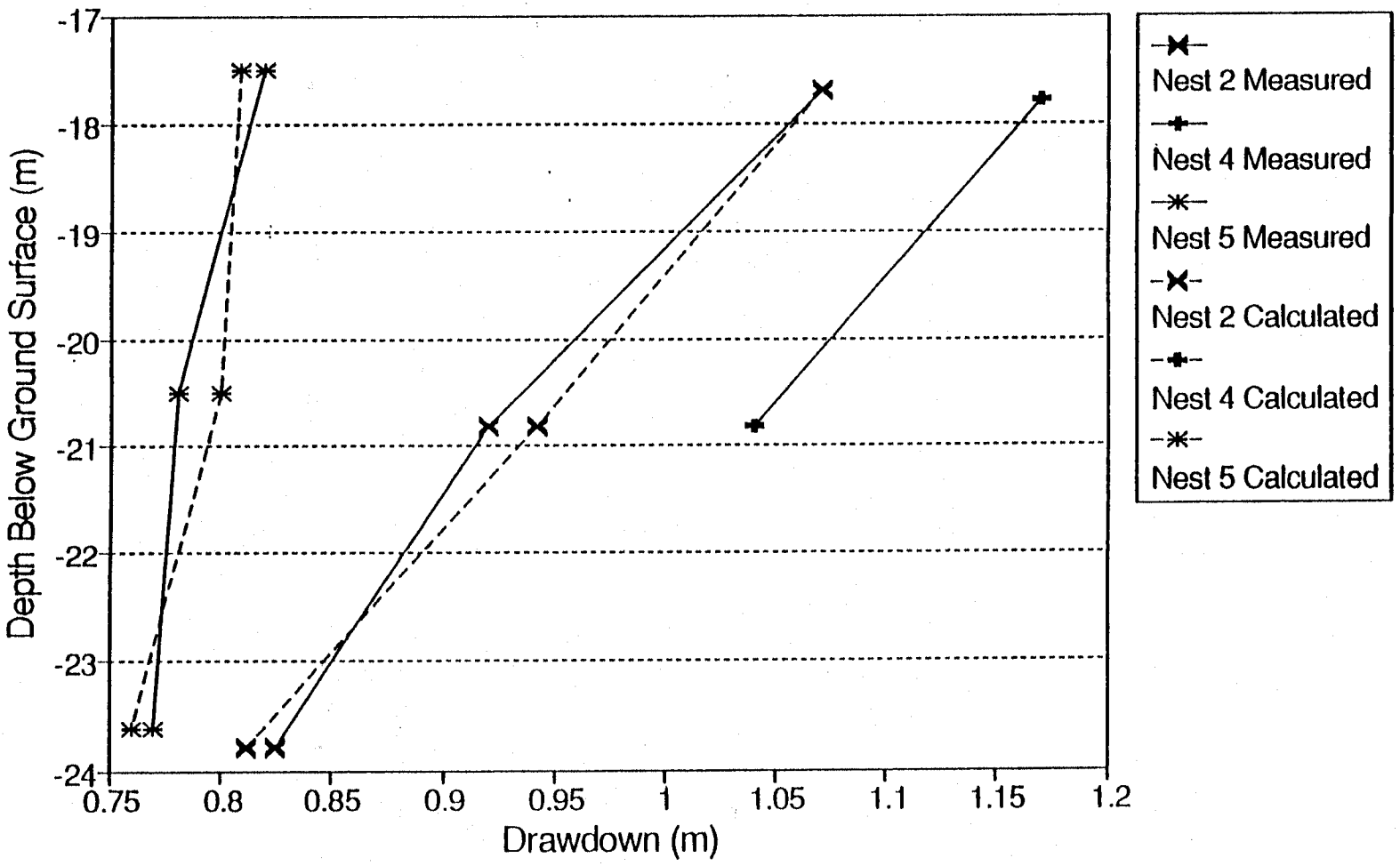

Figure 16: Measured and Calculated Drawdown for the Lower Portion of Test B Calculated Drawdown is based on Fitting to Test B Data

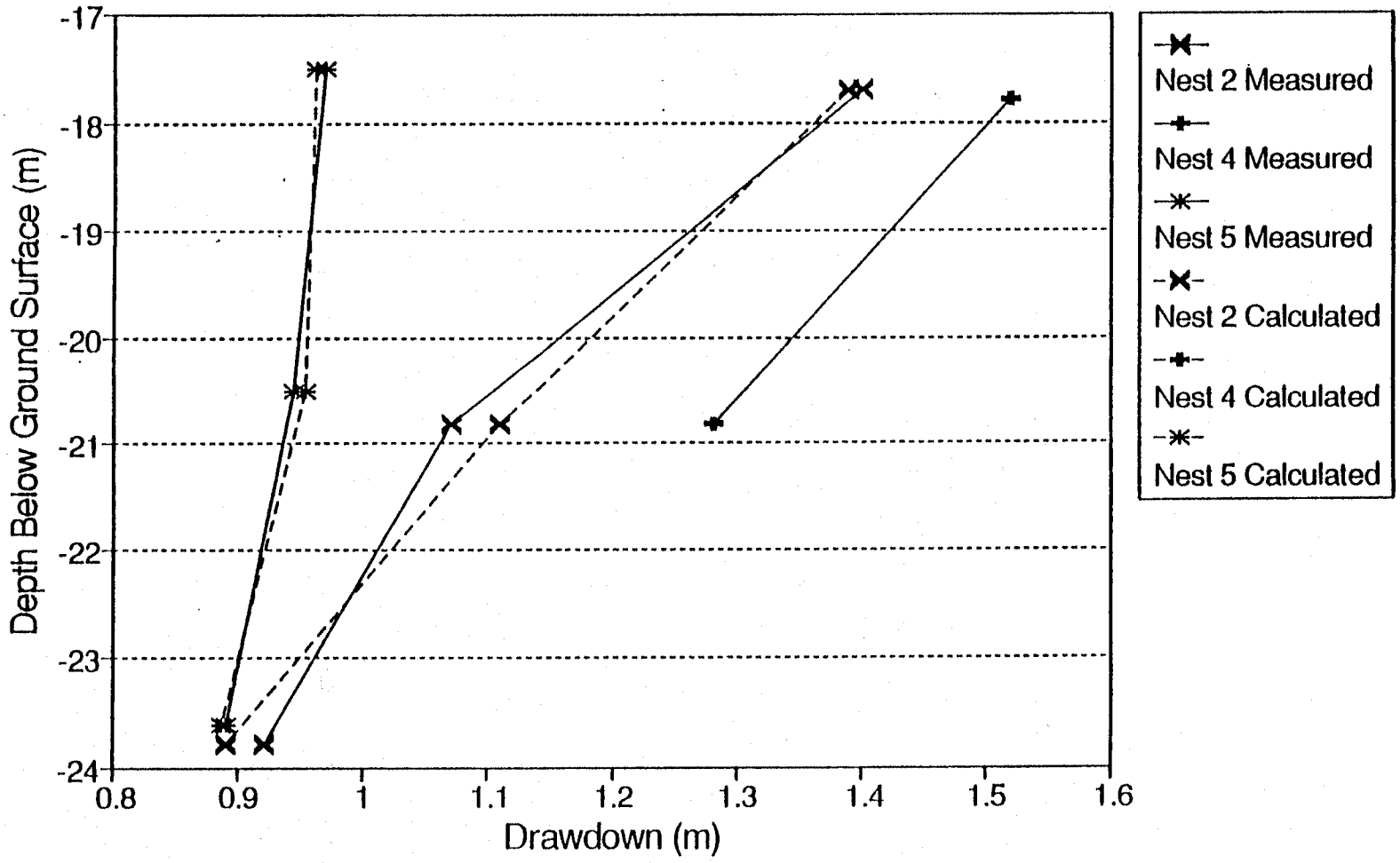

Figure 17: Measured and Calculated Drawdown for the Lower Portion of Test D Calculated Drawdown is based on Fitting to Test D Data

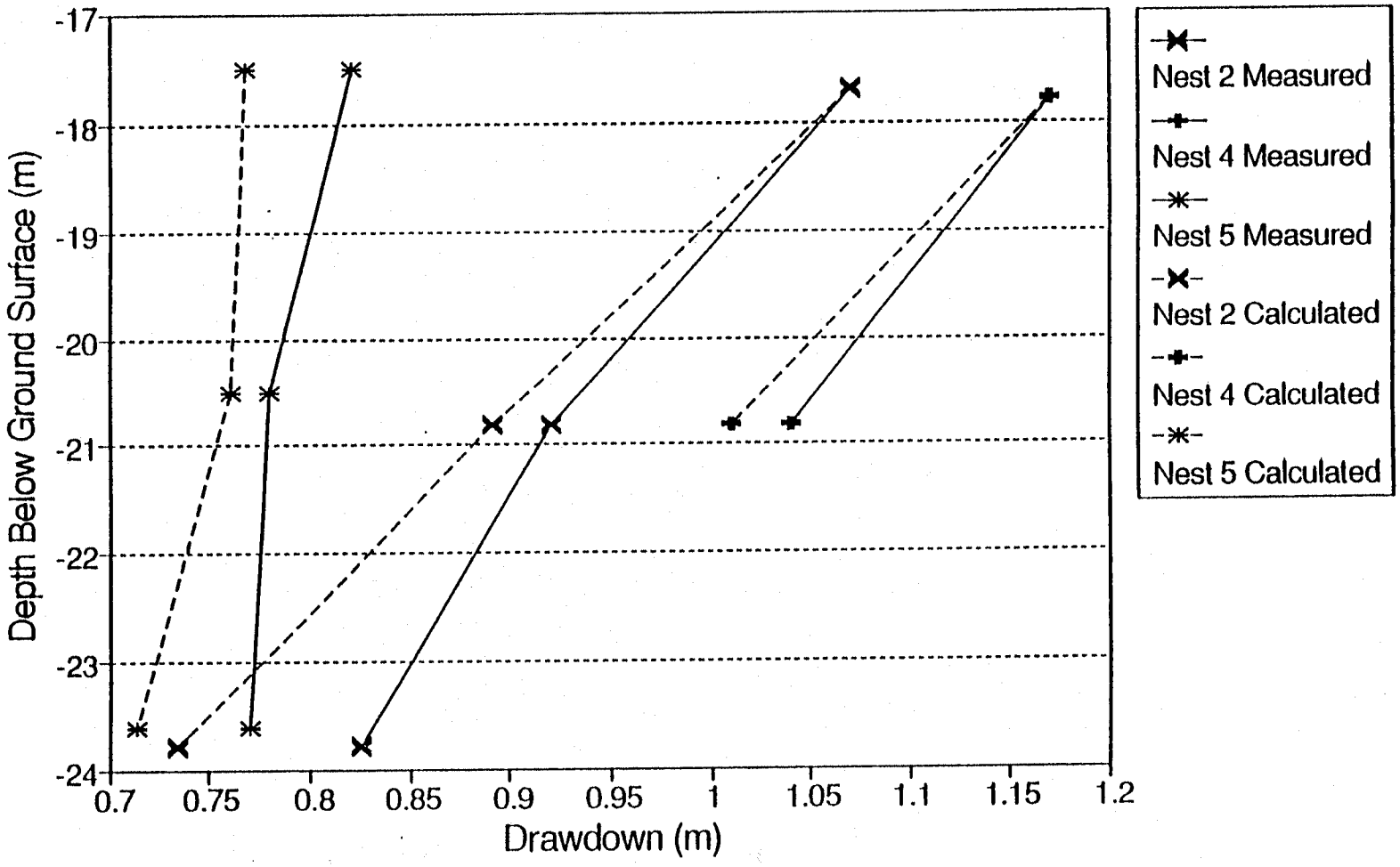

Figure 18: Measured and Calculated Drawdown for the Lower Portion of Test B Calculated Drawdown is based on Fitting to Test B and Test D Data

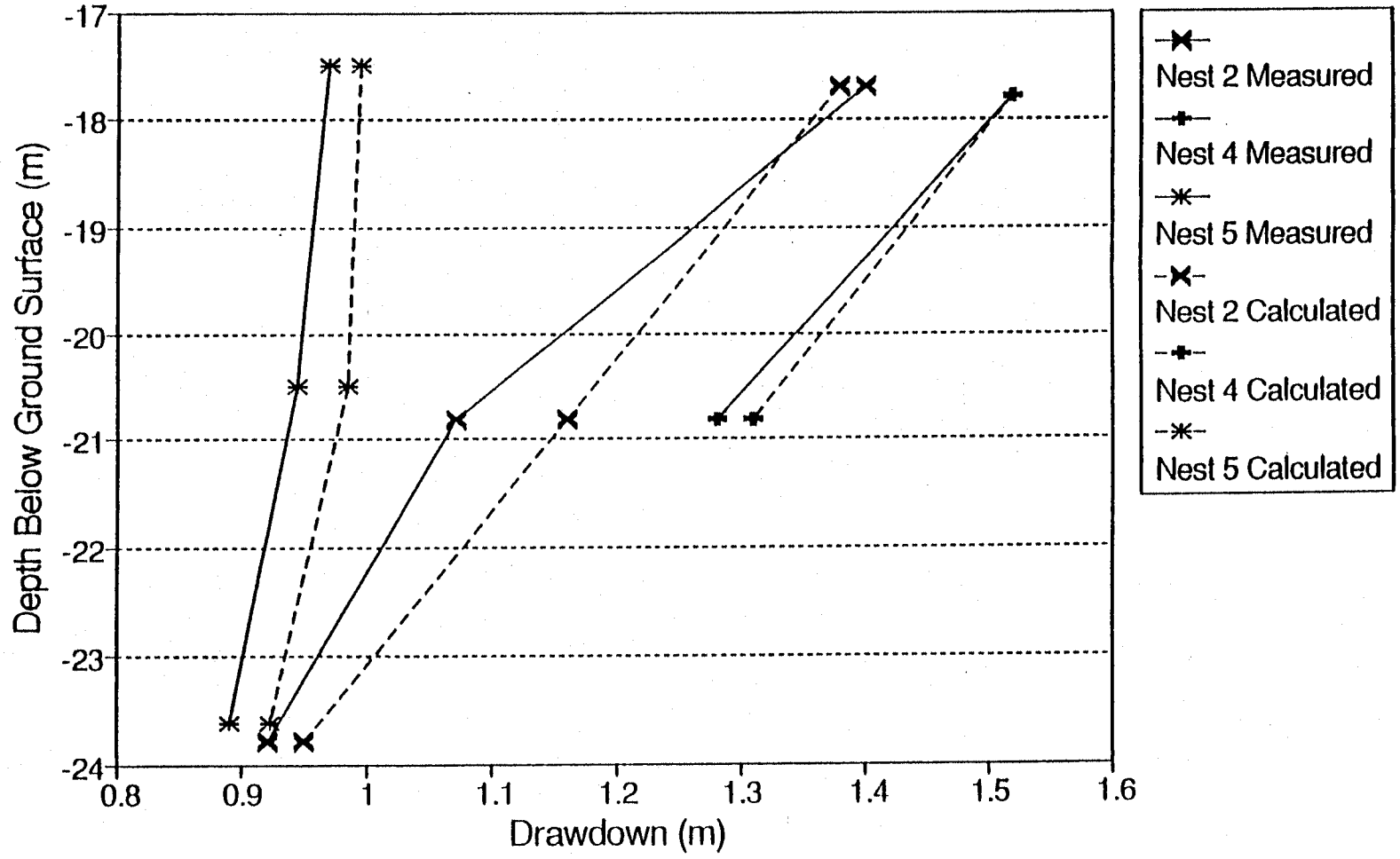

Figure 19: Measured and Calculated Drawdown for the Lower Portion of Test D Calculated Drawdown is based on Fitting to Test B and Test D Data

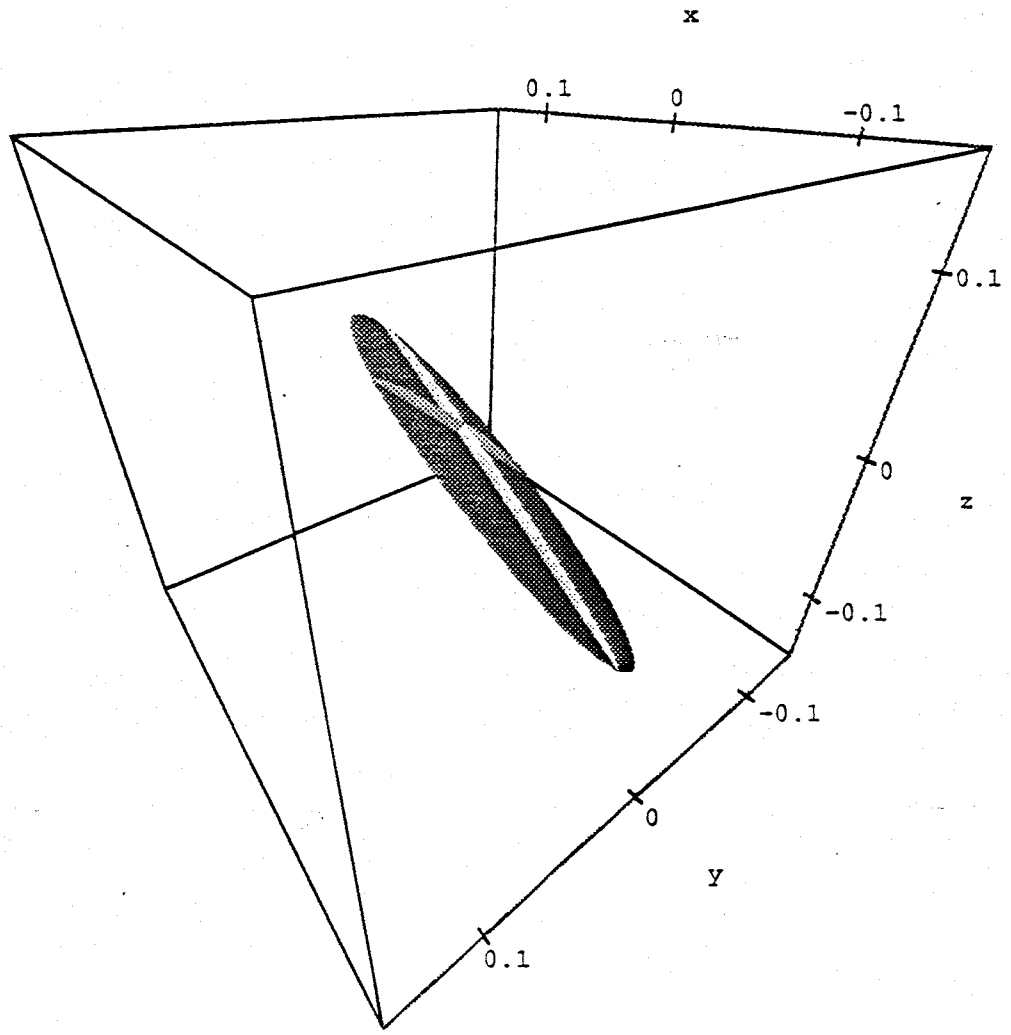

Figure 20: Ellipsoid For Upper Layer Based on Data From Test A

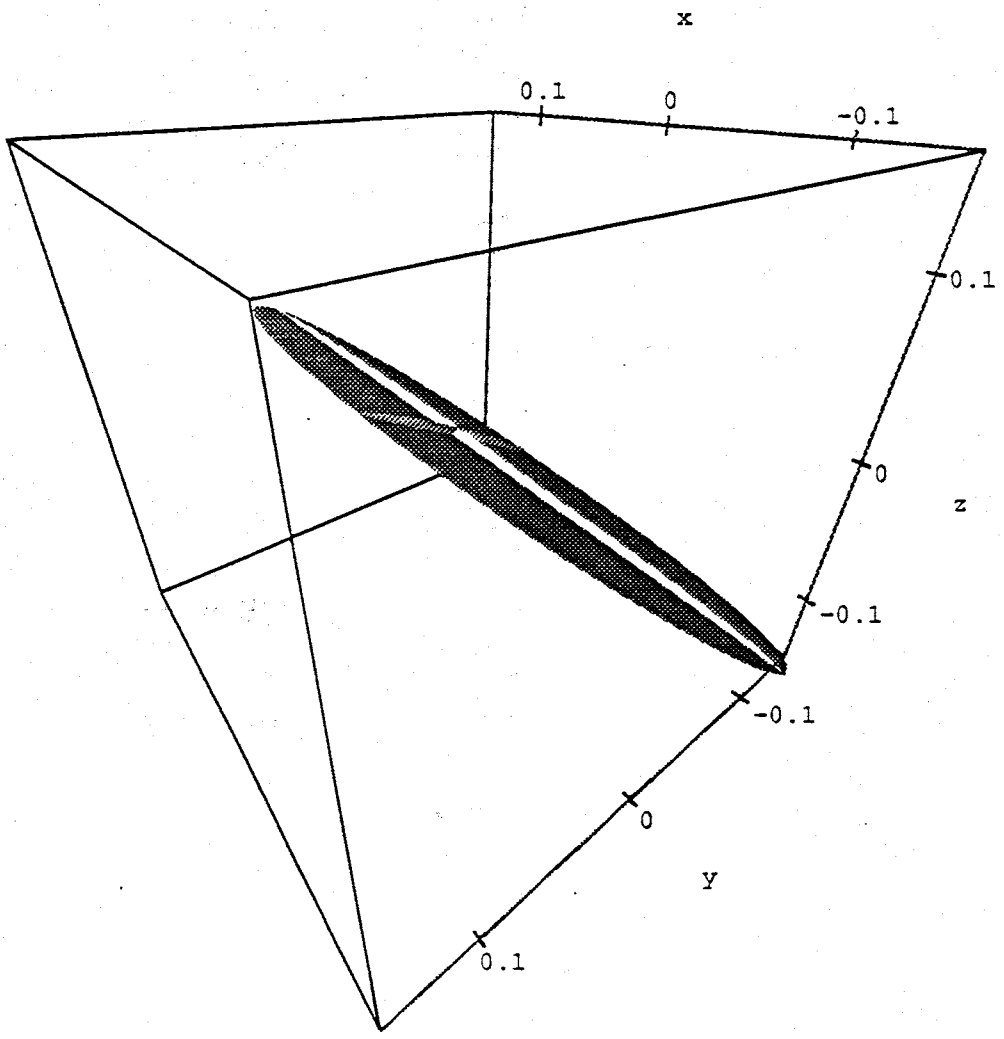

Figure 21: Ellipsoid For Upper Layer Based on Data From Test E

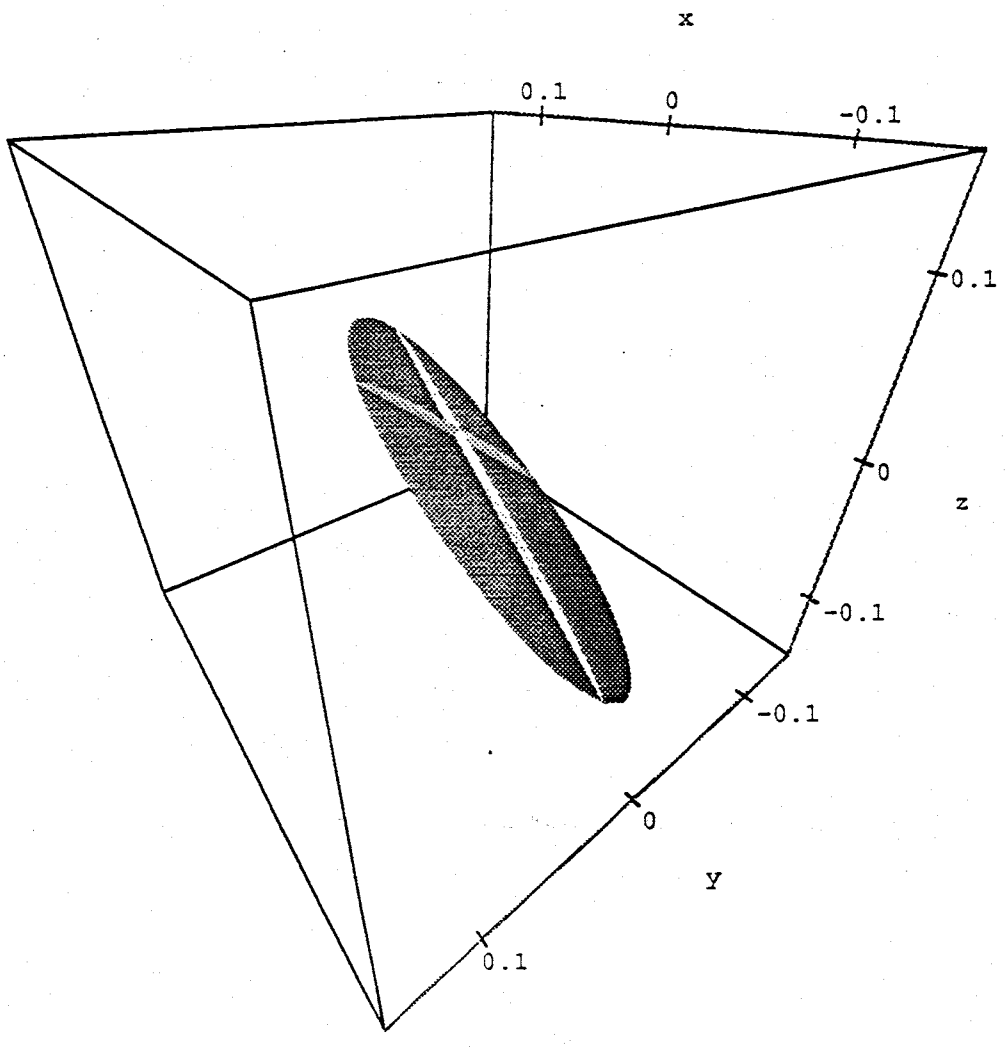

Figure 22: Ellipsoid For Upper Layer Based on Data From Tests A and E

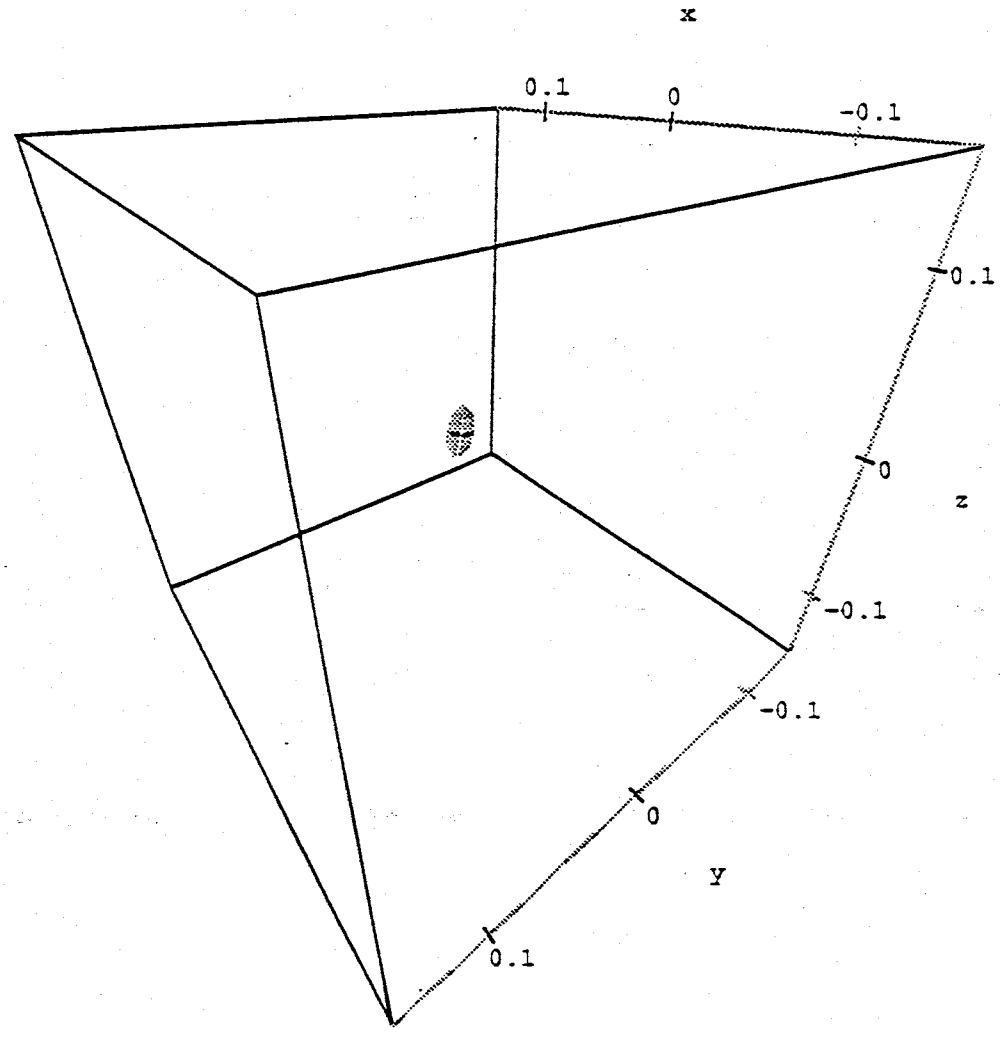

Figure 23: Ellipsoid For Lower Layer Based on Data From Test C

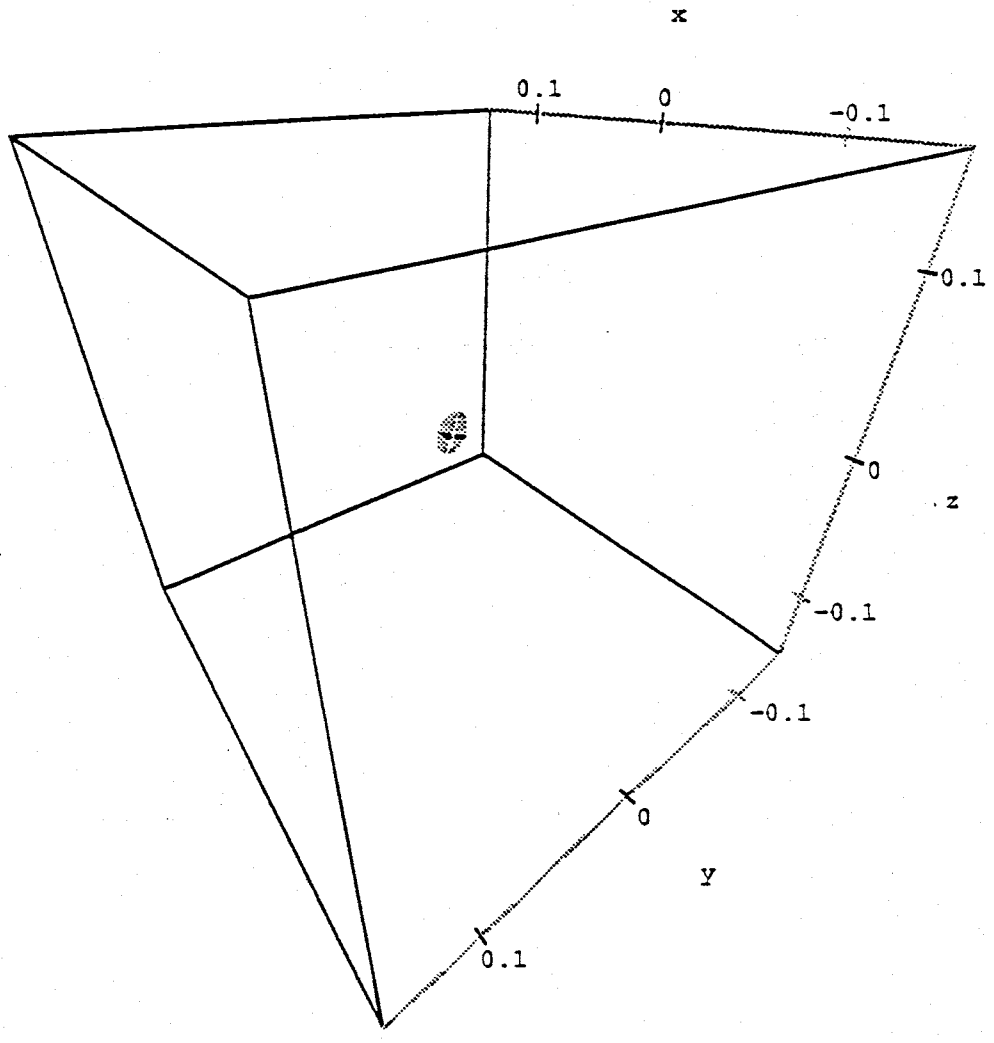

Figure 25: Ellipsoid For Lower Layer Based on Data From Tests C and D

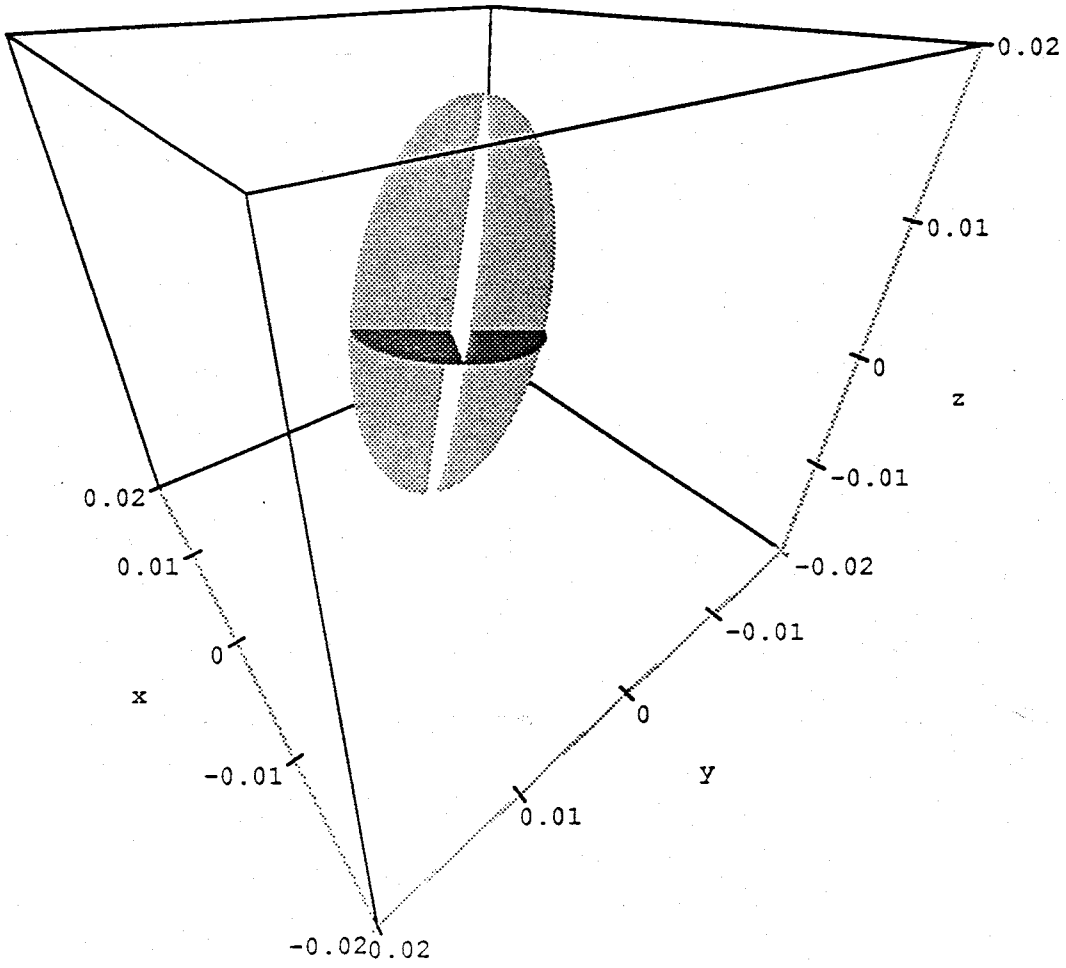

Figure 26: Close-Up of Ellipsoid for Lower Layer Based on Data From Test C

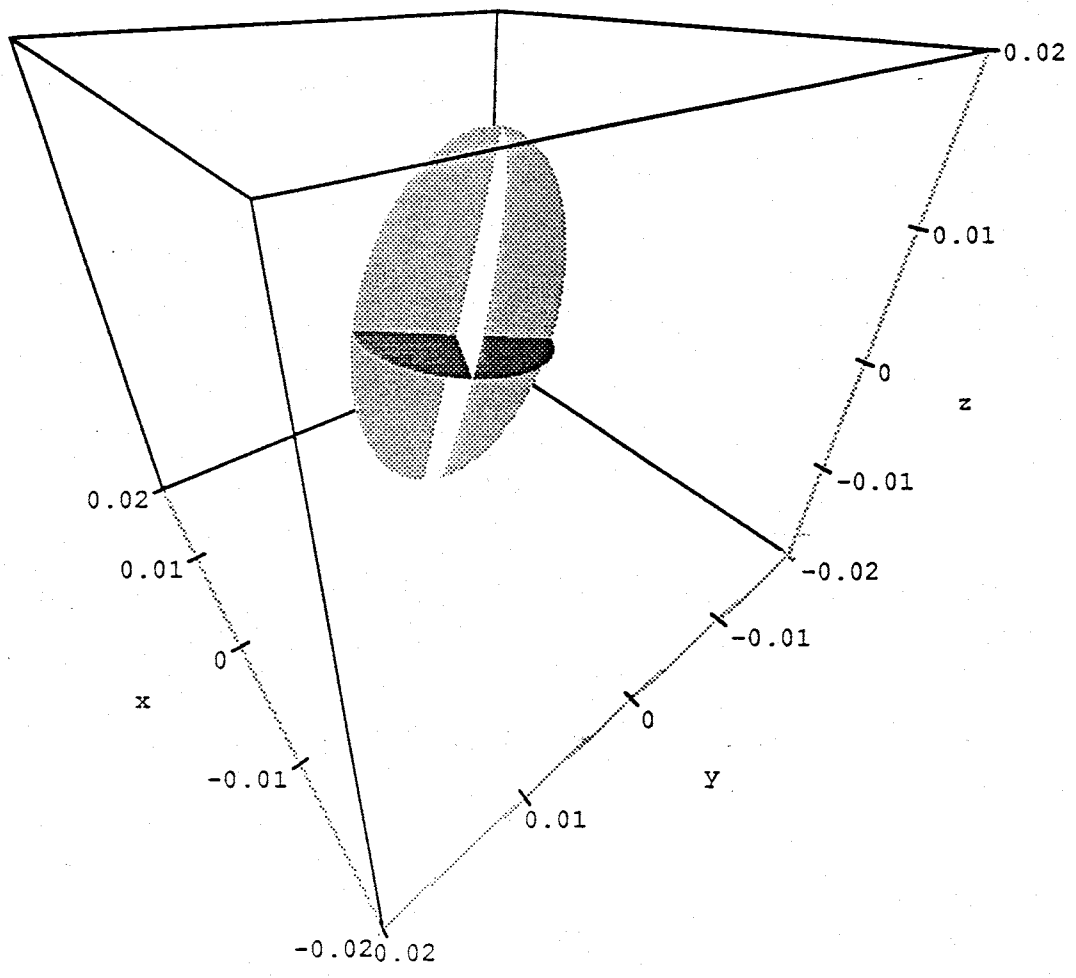

Figure 27: Close-Up of Ellipsoid for Lower Layer Based on Data From Test C and D

DISCUSSION OF RESULTS OF DATA ANALYSIS

From Table 2 we see that the magnitudes of the principal conductivities for the upper layer are similar for the analyses of Tests A and E with Test A having $K_1=3.66X10^{-2}$ m/s, $K_2=4.20X10^{-3}$ m/s, $K_3=2.54X10^{-4}$ m/s; and Test E having $K_1=3.73X10^{-2}$ m/s, $K_2=3.71X10^{-3}$ m/s, $K_3=4.12X10^{-5}$

The directions of the principal conductivities in these two analyses would seem, at first, to be significantly different, but Figures 20 to 22 show that the orientations of the ellipsoids are about the same. As expected, the analysis using the combined data from Tests A and E produced results somewhere between the results of the individual analyses.

From the geological evidence, we have no reason to believe there is significant tilting of the bedding planes; still, K_2 has a dip angle of up to 43° from the horizontal. It's possible that this large angle is the result of heterogeneity in the aquifer. Because Test A and E were performed with only a one foot difference between the depths of the pumped interval, a comparison of the tests would be unlikely to show significantly different results; even if the aquifer is heterogeneous. Another possibility is that this apparent tilt is caused by flow in the well bore below the packer (Figure 11). If the vertical direction is the smallest principal direction, which would be the expected case for this Holocene alluvium, then flow in the well bore would

Table 2:. Results of Data Analysis for Preliminary Pumping Tests.

TESTS ANALYZED	LAYER ANALYZED	K11 (m/s)	K12 (m/s)	K13 (m/s)	K22 (m/s)	K23 (m/s)	K33 (m/s)	PRINCIPAL HYDRAULIC CONDUCTIVITIES (m/s)	DIRECTION
A	UPPER	3.56E-02	-3.12E-3	4.81E-3	3.46E-3	1.37E-3	1.71E-3	K1 = 3.66E-2 K2 = 4.20E-3 K3 = 2.54E-4	E5S v=+6 E89N v=+29 E72N v=-59
E	UPPER	2.50E-2	-7.21E-3	1.31E-3	4.27E-3	1.51E-3	1.76E-3	K1 = 2.73E-3 K2 = 3.71E-3 K3 = 4.12E-5	E17S v=+2 E74N v=+43 E71N v=-47
A and E	UPPER	2.80E-2	-1.01E-2	4.8E-4	6.20E-3	2.01E-3	1.65E-3	K1 = 3.20E-2 K2 = 4.42E-3 K3 = 2.81E-5	E22S v=-1 E68N v=+38 E69N v=-52
B	LOWER	3.14E-5	1.37E-5	-1.8E-5	5.09E-5	-2.32E-5	2.91E-4	K1 = 2.95E-4 K2 = 5.45E-5 K3 = 2.42E-5	E53N v=-83 E64N v=+7 E26S v=+14
D	LOWER	4.57E-5	1.31E-5	-2.87E-5	5.92E-5	2.33E-5	2.10E-4	K1 = 2.19E-4 K2 = 5.95E-5 K3 = 3.66E-5	E42N v=-77 E65N v=+12 E26S v=+5
B and D	LOWER	3.92E-5	1.37E-5	2.4E-5	5.64E-5	-2.39E-5	2.37E-4	K1 = 2.43E-4 K2 = 5.82E-5 K3 = 3.11E-5	E47N v=-79 E65N v=+10 E26S v=+3

have it's greatest impact on the deepest points, where as drawdown from the point sink is at a minimum. Drawdown, due to flow in the well bore, would also be greater in the piezometers nearer to the well bore. The result of this higher drawdown at the deep points, near the well bore would be an apparent higher hydraulic conductivity in the direction of these points. This is precisely what we see in the results from Tests A and E where K_2 is directed down in the direction of the nests nearest to the center (2 and 4).

From Table 2, we can see that the magnitudes of the principal conductivities determined for the lower layer, from the analyses of Tests C and D are also about the same. Figures 23 to 27 show that the ellipsoids from these analyses also have roughly the same orientation. In contrast to the results from the upper layer, where the principal conductivities ranged over three orders of magnitude, the results from the lower layer are within an order of magnitude of each other; suggesting that the lower layer is much less anisotropic than the upper layer. It should also be noted that the largest principal hydraulic conductivity in the upper layer is two orders of magnitude larger than the largest principal hydraulic conductivity in the lower layer, which agrees with the fact that the maximum drawdown in the lower layer tests were five times greater than the maximum drawdown in the upper layer tests. From the geology of the region, we would expect the lower layer would also have it's smallest principal hydraulic conductivity in the vertical direction. In the results of the analysis for the lower layer, there

is a principal direction that is almost vertical, but it has the largest hydraulic conductivity. This may also be due to flow in the well bore below the packer, causing higher drawdown at the deeper points. The absence of significant tilting is a result of the more isotropic conditions.

CONCLUSIONS AND RECOMMENDATIONS

From the results of the tests performed so far, we have determined that there are at least two distinct layers separated by a low hydraulic conductivity layer. Overall, the upper layer has a higher hydraulic conductivity, but is more anisotropic than the lower layer. No conclusive statement can be made about the actual values of hydraulic conductivity in either layer due to the unresolved questions of heterogeneity and flow in the well bore.

The first step in resolving these questions should be more pumping tests with the pumped interval at more varied depths. If the theory of flow in the well bore is correct, then results from the upper layer should show the angle of tilt varying with the depth of the packer. If heterogeneity is in fact the cause of tilt, then pumping tests with the pumping interval at different depth should show no correlation. If similar results are produced from more tests, then these results could be taken as locally correct and attributed to unknown geologic conditions. If, in fact, flow in the well bore is having a significant affect, then the problem can be overcome by placing more packers at various depths above and below the pumped interval to eliminate the well bore as a flow path. If this approach is taken, then commercial packers should be used because with more packers, reliability will become a key issue.

Overall, the tests performed so far have produced useful information in characterizing the aquifer being studied. They have also given the direction future tests must take to more accurately and definitively characterize the aquifer.

REFERENCES

Boulton, N.S.,1954, "The Drawdown of a Water-Table Under Non-Steady Conditions Near a Pumped Well in an Unconfined Formation": Proceedings of the Institute of Civil Engineering, Volume 3, No. 3, pp. 564-579.

Carslaw, H.E., and Jaeger, J.C., 1959, Conduction of Heat in Solids: Oxford University Press, New York.

Driscoll, Fletcher G., 1986, Groundwater and Wells, pp. 537-541: Johnson Division, St. Paul, Minnesota.

Hantush, M.S., 1964, Hydraulics of wells, Advances in Hydroscience, edited by Ven T. Chow: Academic Press, New York and London, Volume 1, pp. 282-430.

Hantush, M.S., 1966, "Wells in Homogeneous Anisotropic Aquifers": Water Resources Research, Volume 2, No. 2, pp. 273-279.

Hantush, M.S., 1966, "Analysis of Pumping Tests in Anisotropic Aquifers": Journal of Geophysical Research, Volume 71, No. 2, pp. 421-426.

Hsieh, P.A., and Neuman, S.P., 1985, "Field Determination of Three-Dimensional Hydraulic conductivity Tensor of Anisotropic Media, 1. Theory": Water Resources Research, Volume 21, Nor. 11, pp. 1655-1665.

Neuman, S.P., 1972, Theory of Flow in Unconfined Aquifers Considering Delayed Response of the Water Table: Water Resources Research, Volume 8, No. 4, pp. 1031-1045.

Neuman, S.P., Walter, G.R., Bentley, H.W., Ward, J.J., and Gonzalez, D.D., 1984, Determination of Horizontal Aquifer Anisotropy with Three Wells: Ground Water, Volume 22, No. 1, pp. 66-72.

Papadopulos, I.S., 1965, Non-Steady Flow to a Well in an Infinite Anisotropic Aquifer: Proceedings of the Dubrovnik Symposium on Hydrology of Fractured Rocks, International Association of Scientific Hydrology, pp. 21-31.

Press, William H., Flannery, Brian P., Teukolosky, Saul A., and Vetterling, William T., 1986, Numerical Recipes: The Art of Scientific Computing, Cambridge University Press, New Rochelle, New York, pp. 498-538.

Streltsova, T.D., 1972, Un-Steady Radial Flow in an Unconfined Aquifer: Water Resources Research, Volume 8, No. 4, pp. 1059-1066.

Way, S.C., and Mckee, C.R., 1982, In-Situ Determination of Three-Dimensional Aquifer Permeabilities: Groundwater, Volume 20, No. 5, pp. 594-603.

Weeks, E.P., 1969, Determining the Ratio of Horizontal to Vertical Permeability by Aquifer-Test Analysis: Water Resources Research, Volume 5, No. 1, pp. 196-214.

Zody, S.P., 1989, Seismic Refraction Investigation of the Shallow Subsurface of the Lower Rio salado, Northwest of San Acacia, New Mexico: Unpublished Thesis, New Mexico Institute of Mining and Technology.

APPENDIX

FORTRAN CODE FOR DETERMINING THE LEAST SQUARED ERROR CONDUCTIVITY TENSOR TO MATCH PUMP TEST DATA

```
****** This program computes the hydraulic conductivity
****** tensor, principal values and vectors from steady
****** state pumping test data, with a point sink and
****** point observations.At least 6 observations are
****** required.The data file must have the following
****** form (all units are in meters and seconds)
******
****** nt
****** np ba d q l wt
****** X Y Z s
******   .
******   .
******   .
****** np ba d q l wt
******
****** nt=number of tests in data file
****** np= number of data points in a test
****** ba=aquifer thickness
****** d=depth to center of pumped interval(negative)
****** l=length of pumped interval
****** wt=depth to upper boundary (negative)
****** X Y Z=coordinates of the observation point wrt top center of
****** pumping well
****** s=drawdown at X Y Z
****** Other input variables include:
****** maxiter=maximum number of iterations
****** number of image well iterations=number of
****** image wells to be used for the case of an
****** upper and lower boundary.Enter 0 for upper
****** boundary only
******
****** epsilon=convergence criterion (~standard deviation)
****** xkij=initial guesses of conductivity
****** The output file includes:
****** rms=root mean square error
****** final values of xk
****** standard error of estimation(sigma) for xk
****** principal values of conductivity
****** principal vectors
****** measured drawdown calculated drawdown and the
****** difference for each point

      implicit double precision(a-h,q-z)
      dimension hm(50,50),hc(50,50),xk(6,6),derh(6),xkl(6,6)
     c,a(6,6),b(6),x(50,50,3),xp(6),hcl(50,50),np(50),alph(50,50)
     c,q(50),xl(50),ba(50),d(50),eva(3),eve(3,3),c(6,6)
     c,wt(50),xz(50,50)
      character*10 infil,outfil
      character*20 titl
      xpi=3.141593
      write(*,*)'enter 1 to skip description 2 for description'
      read(*,*)iskp
      if(iskp .eq. 1)go to 5
      write(*,*)'This program computes the hydraulic conductivity'
      write(*,*)'tensor principal values and vectors from steady'
      write(*,*)'state pumping test data with a point sink and'
      write(*,*)'point observations.At least 6 observations are'
      write(*,*)'required.The data file must have the following'
      write(*,*)'form (all units are in meters and seconds'
      write(*,*)'enter 1 to continue'
```

```
      read(*,*) itst
      write(*,*)'nt'
      write(*,*)'np ba d q l wt'
      write(*,*)'X Y Z s'
      write(*,*)'  .'
      write(*,*)'  .'
      write(*,*)'  .'
      write(*,*)'np ba d q l wt'
      write(*,*)'nt=number of tests in data file'
      write(*,*)'np= number of data points in a test'
      write(*,*)'ba=aquifer thickness'
      write(*,*)'d=depth to center of pumped interval(negative)'
      write(*,*)'q=pumping rate'
      write(*,*)'l=length of pumped interval'
      write(*,*)'wt=depth to upper boundary (negative)'
      write(*,*)'X Y Z=coordinates of observation point'
      write(*,*)'s=drawdown at X Y Z'
      write(*,*)'enter 1 to continue'
      read(*,*)itst
      write(*,*)'Other input variables include:'
      write(*,*)'maxiter=maximum number of iterations'
      write(*,*)'number of image well iterations=number of'
      write(*,*)'image wells to be used for the case of an'
      write(*,*)'upper and lower boundary.Enter 0 for upper'
      write(*,*)'boundary only'
      write(*,*)' '
      write(*,*)'epsilon=convergence criterion (~standard deviation)'
      write(*,*)'xkij=initial guesses of conductivity'
      write(*,*)'The output file includes:'
      write(*,*)'rms=root mean square error'
      write(*,*)'final values of xk'
      write(*,*)'standard error of estimation(sigma) for xk'
      write(*,*)'principal values of conductivity'
      write(*,*)'principal vectors'
      write(*,*)'measured drawdown calculated drawdown and the'
      write(*,*)'difference for each point'
 5    continue
      write(*,*)'enter 1 to exit 2 to continue'
      read(*,*)ix
      if(ix .eq. 1)go to 380
      write(*,*) 'enter data file to be used'
      read(*,*) infil
      write(*,*)'enter output file'
      read(*,*)outfil
      open(unit=20,file=outfil,status='new')
      write(*,*)'enter title'
      read(*,*)titl
      write(20,*)titl
      write(*,*)'write maxiter'
      read(*,*)itmax
      write(*,*)'enter number of image well iterations'
      read(*,*)ni
      open(unit=10,file=infil,status='old')
* read data
      read(10,*)nt
      do 12 it=1,nt
        read(10,*)np(it),ba(it),dp,q(it),xl(it),wt(it)
        d(it)=wt(it)-dp
        do 10 ih=1,np(it)
          tot=tot+1
```

```
          read(10,*)x(it,ih,1),x(it,ih,2),xz(it,ih),hm(it,ih)
          x(it,ih,3)=xz(it,ih)-dp
 10       continue
 12     continue
*  read parameters
       write(*,*) 'enter epsilon(~experimental standard deviation)'
       read(*,*) eps
       teps=.1*eps**2
       write(*,*)'enter initial guesses'
       write(*,*)'xk11'
       read(*,*)xk(1,1)
       write(*,*)'xk22'
       read(*,*)xk(2,2)
       write(*,*)'xk33'
       read(*,*)xk(3,3)
       write(*,*)'xk12'
       read(*,*)xk(1,2)
       write(*,*)'xk13'
       read(*,*)xk(1,3)
       write(*,*)'xk23'
       read(*,*)xk(2,3)
       xk(3,1)=xk(1,3)
       xk(2,1)=xk(1,2)
       xk(3,2)=xk(2,3)
       xlam1=.01
       write(20,*)' '
       write(20,*)'Initial values of parameters'
       write(20,340) xk(1,1),xk(2,2),xk(3,3)
*  calculate drawdown using parametrs
 20    continue
       do 35 it=1,nt
         do 30 idd=1,np(it)
           x1=x(it,idd,1)
           x2=x(it,idd,2)
           x3=x(it,idd,3)
           ba1=ba(it)
           q1=q(it)
           d1=d(it)
           xl1=xl(it)
           call  dd(xk,ba1,q1,d1,x1,x2,x3,ni,xl1,alphx,hcx)
           alph(it,idd)=alphx
           hc(it,idd)=hcx
 30        continue
 35      continue
*  calculated error
       errnu=rsqerr(hm,hc,nt,np,tot)
*  test error
       write(*,*)'ernu=',errnu
       if(abs(err3-errnu).le.teps) then
         istat=1
         endif
       if(iter.ge.itmax) then
         istat=3
         endif
       iter=iter+1
       write(*,*)'iterations=',iter
       do 50 iz=1,6
         b(iz)=0
         do 40 jz=1,6
           a(iz,jz)=0
```

```
 40        continue
 50      continue
*  calculated array
       do 85 it=1,nt
         do 80 ia=1,np(it)
           hh=(hm(it,ia)-hc(it,ia))
           x1=x(it,ia,1)
           x2=x(it,ia,2)
           x3=x(it,ia,3)
           ba1=ba(it)
           q1=q(it)
           d1=d(it)
           call derv(xk,ba1,q1,d1,x1,x2,x3,ni,derh)
           do 70 ja=1,6
             b(ja)=b(ja)+derh(ja)*hh
             do 60 ka=ja,6
               a(ja,ka)=a(ja,ka)+derh(ja)*derh(ka)
               a(ka,ja)=a(ja,ka)
 60            continue
 70          continue
 80        continue
 85      continue
       if(istat .ne.0)go to 140
*  add lamda to diagonal terms
 90    do 100 is=1,6
         a(is,is)=a(is,is)*(1+xlam1)
 100     continue
*  solve new array
       call dlsarg(6,a,6,b,1,xp)
       ic=0
       do 120 iu=1,3
         do 110 ju=iu,3
           ic=ic+1
           if(iu .eq. ju)then
             xk1(iu,ju)=abs(xk(iu,ju)+xp(ic))
             else
             xk1(iu,ju)=xk(iu,ju)+xp(ic)
             xk1(ju,iu)=xk1(iu,ju)
             endif
 110       continue
 120     continue
       do 132 it=1,nt
         do 130 jdd=1,np(it)
           x1=x(it,jdd,1)
           x2=x(it,jdd,2)
           x3=x(it,jdd,3)
           ba1=ba(it)
           q1=q(it)
           d1=d(it)
           xl1=xl(it)
           call dd(xk1,ba1,q1,d1,x1,x2,x3,ni,xl1,alph1,hc1x)
           hc1(it,jdd)=hc1x
 130       continue
 132     continue
       err2=rsqerr(hm,hc1,nt,np,tot)
*  test new error
       if(err2 .lt. errnu) then
*    reduce lamda and start next iteration
         xlam1=xlam1/2.
         do 135 ik=1,3
```

```
          do 133 jk=1,3
            xk(ik,jk)=xkl(ik,jk)
 133        continue
 135      continue
        err3=errnu
        errnu=err2
        go to 20
        else
* increase lamda and try again
        xlaml=xlaml*1.2
        write(*,*)'lamda=',xlaml
        if(xlaml .gt.300)then
          istat=2
          go to 140
          endif
        go to 90
        endif
 140  continue
**calculate root mean square error**
      rms=dsqrt(errnu/tot)
**calculate covariance matrix**
      call dlinds(6,a,6,c,6)
**calculate principal values and vectors**
      call devcsf(3,xk,6,eva,eve,3)
      do 150 io=1,3
        write(*,*)xk(io,1),xk(io,2),xk(io,3)
 150    continue
      write(*,*)'stat=',istat,'iter=',iter,'rms',rms,'ni',ni
**output results**
      write(20,*)' '
      if(istat .eq. 1) write(20,*)'**Program succeeded**'
      if(istat .eq. 3) write(20,*)'**Failed to converge in',itmax,
     c'iterations**'
      if(istat .eq. 2) write(20,*)'**Failed to converge,lamda
     cgreater than 100.**'
      write(20,*)' '
      write(20,*)'Final values'
      ic=0
      do 160 nop=1,3
        do 155 nop2=nop,3
          ic=ic+1
          write(20,300)'K',nop,nop2,xk(nop,nop2),'sigma',
     c    rms*dsqrt(c(ic,ic))
 155      continue
 160    continue
      write(20,*)
      write(20,*)'aquifer thickness =',ba(1)
      write(*,*)'aquifer thickness =',ba(1)
      write(20,*)
      write(20,310)rms,ni*4+1
      write(20,*)
      write(20,*)
      do 165 ie=1,3
        write(20,360)ie,eva(ie)
        write(*,360)ie,eva(ie)
        write(20,370)ie,eve(1,ie),eve(2,ie),eve(3,ie)
        write(*,370)ie,eve(1,ie),eve(2,ie),eve(3,ie)
 165    continue
      write(20,*)
      write(20,320)'x1','x2','x3','h actual','h calc','difference '
```

```
     c,'alph'
      do 180 it=1,nt
        do 170 ip=1,np(it)
          write(20,330)x(it,ip,1),x(it,ip,2),xz(it,ip),
     c     hm(it,ip),hc(it,ip), hm(it,ip)-hc(it,ip),alph(it,ip)
 170      continue
 180    continue
 300   format(a2,i2,i2,3x,e9.3,3x,a6,e9.3)
 310   format('RMS error='e9.3,'number of image wells',i7)
 320   format(a11,a11,a11,a11,a11,a11,a11)
 330   format(e9.3,'  ',e9.3,'  ',e9.3,'  ',e9.3,'  ',e9.3,'  ',e9.3,
     c'  ',e9.3)
 340   format(e9.3,' ',e9.3,' ',e9.3)
 350   format(i4,e9.3,e9.3,e9.3)
 360   format('eigenvalue',i1,'=',e9.3)
 370   format('eigenvector',i1,'= ',e9.3,2x,e9.3,2x,e9.3)
 380   continue
       stop
       end



**************************************
**   calculate square error         **
**            input                 **
**  h1 and h2 two data sets         **
**  nt=number of tests              **
**  np=number of points in eachtest **
**        returns                   **
**  squared error                   **
**************************************
       function rsqerr(h1,h2,nt,np,tot)
       implicit double precision(a-h,q-z)
       dimension h1(50,50),h2(50,50),np(50)
       sqerr=0
       do 150 it=1,nt
         do 100 i=1,np(it)
           sqerr= sqerr+((h1(it,i)-h2(it,i)))**2
 100       continue
 150     continue
       rsqerr=sqerr
       return
       end




**********************************************************
**  calculate partial derivatives of drawdown           **
**  input:                                              **
**        xk=conductivity array                         **
**        b=aquifer thickness                           **
**        q=pumping rate                                **
**        d=distance from point sink to boundary        **
**        x1,x2,x3=coordinates of observation point     **
**        ni=number of image well iterations            **
**    output:                                           **
**         derh=partial derivatives                     **
**********************************************************
```

```
      subroutine derv(xk,b,q,d,x1,x2,x3,ni,derh)
      implicit double precision(a-h,q-z)
      dimension xk(6,6),x(6,6),gxx1(6,6),gxx2(6,6),d1(2),ak(6,6)
     c,derh(6),dg(6),ddet(6),xt(6,6)
      xpi=3.1415926536
      x(1,1)=x1
      x(2,1)=x2
      x(3,1)=x3
      xt(1,1)=x1
      xt(1,2)=x2
      xt(1,3)=x3
**calculate gxx**
      call adjoint(xk,det,ak)
      call amult(xt,1,3,ak,3,gxx1)
      call amult(gxx1,1,3,x,1,gxx2)
      gxx=gxx2(1,1)
**calculate partial derivatives of gxx**
      dg(1)=x2**2*xk(3,3)+x3**2*xk(2,2)-2*x2*x3*xk(2,3)
      dg(4)=x1**2*xk(3,3)+x3**2*xk(1,1)-2*x1*x3*xk(1,3)
      dg(6)=x1**2*xk(2,2)+x2**2*xk(1,1)-2*x1*x2*xk(1,2)
      dg(2)=2*x1*x3*xk(2,3)+2*x2*x3*xk(1,3)-2*x3**2*xk(1,2)
     c-2*x1*x2*xk(3,3)
      dg(3)=2*x1*x2*xk(2,3)+2*x2*x3*xk(1,2)-2*x2**2*xk(1,3)
     c-2*x1*x3*xk(2,2)
      dg(5)=2*x1*x2*xk(1,3)+2*x1*x3*xk(1,2)-2*x1**2*xk(2,3)
     c-2*x2*x3*xk(1,1)
**calculate partial derivatives of detrminate/xk33**
      ddet(1)=(xk(2,2)*xk(3,3)-xk(2,3)**2)/xk(3,3)
      ddet(4)=(xk(1,1)*xk(3,3)-xk(1,3)**2)/xk(3,3)
      ddet(6)=(xk(1,1)*xk(2,2)-xk(1,2)**2)/xk(3,3)
     c-det/(xk(3,3)**2)
      ddet(2)=(2*xk(1,3)*xk(2,3)-2*xk(3,3)*xk(1,2))/xk(3,3)
      ddet(3)=(2*xk(1,2)*xk(2,3)-2*xk(2,2)*xk(1,3))/xk(3,3)
      ddet(5)=(2*xk(1,2)*xk(1,3)-2*xk(1,1)*xk(2,3))/xk(3,3)
**calculate partial derivatives of drawdown**
      do 40 id=1,6
        derh(id)=1/dsqrt(gxx)**3*dg(id)
     c  +1/dsqrt(gxx+4*det*d*(d-x3)/xk(3,3))**3
     c  *(dg(id)+ddet(id)*4*d*(d-x3))
        do 20 i=1,ni
          do 15 idd=1,2
            d1(1)=(-1)**idd*i*b+d
            d1(2)=(-1)**idd*i*b
            do 10 j=1,2
              derh1=1/dsqrt(gxx+4*det*d1(j)*(d1(j)-x3)
     c        /xk(3,3))**3*(dg(id)+ddet(id)*4*d1(j)*(d1(j)-x3))
              derh(id)=derh(id)+derh1
 10           continue
 15         continue
 20       continue
          derh(id)=-q*derh(id)/(8*xpi)
 40     continue
      return
      end



**********************************************************
*  calculate  drawdown                                   **
```

```
**  input:                                                    **
**        xk=conductivity array                               **
**        b=aquifer thickness                                 **
**        q=pumping rate                                      **
**        d=distance from point sink to boundary              **
**        x1,x2,x3=coordinates of observation point           **
**        ni=number of image well iterations                  **
**        xl=length of pumped interval                        **
**    output:                                                 **
**         alpha=test for point sink                          **
**         dh=drawdown                                        **
************************************************************

      subroutine dd(xk,b,q,d,x1,x2,x3,ni,xl,alph,dh)
      implicit double precision(a-h,q-z)
      dimension xk(6,6),xx(6,6),gxx1(6,6),gxx2(6,6),dl(2),ak(6,6)
     c,xt(6,6)
      xpi=3.1415926536
      xx(1,1)=x1
      xx(2,1)=x2
      xx(3,1)=x3
      xt(1,1)=x1
      xt(1,2)=x2
      xt(1,3)=x3
**calculate gxx**
      call adjoint(xk,det,ak)
      call amult(xt,1,3,ak,3,gxx1)
      call amult(gxx1,1,3,xx,1,gxx2)
      gxx=gxx2(1,1)
      alph=dsqrt(4*gxx/(ak(3,3)*xl**2))
**calculate drawdown from real well and first image well**
      sg=1/dsqrt(gxx)+1/dsqrt(gxx+4*det*d*(d-x3)/xk(3,3))
**calculate from successive image wells**
      do 30 i=1,ni
        do 20 id=1,2
          dl(1)=(-1)**id*i*b+d
          dl(2)=(-1)**id*i*b
          do 10 j=1,2
            sg1=1/dsqrt(gxx+4*det*dl(j)*(dl(j)-x3)/xk(3,3))
            sg=sg+sg1
 10         continue
 20       continue
 30     continue
      dh=q*sg/(4*xpi)
      return
      end

************************************************************
**  multiply two arrays                                     **
*  matrix c=ab                                             **
* l=number of rows in a                                    **
*  m=number of columns in a = number of rows in b          **
*  n = number of columns in b                              **
************************************************************

      subroutine amult(a,l,m,b,n,c)
      implicit double precision(a-h,q-z)
      dimension a(6,6),b(6,6),c(6,6)
      do 20 i=1,l
        do 10 j=1,n
```

```
          c(i,j)=0
          do 5 k=1,m
            c(i,j)=c(i,j)+a(i,k)*b(k,j)
 5          continue
 10       continue
 20     continue
      return
      end


**********************************************************************
**  calculate adjoint and determinant of conductivity tensor        **
**  input:                                                          **
**        xk=conductivity tensor                                    **
**  output:                                                         **
**        d=determinant of xk                                       **
**        ak=adjoint of xk                                          **
**********************************************************************

      subroutine adjoint(xk,d,ak)
      implicit double precision(a-h,q-z)
      dimension xk(6,6),ak(6,6)
      d=xk(1,1)*xk(2,2)*xk(3,3)+2*xk(1,3)*xk(2,3)*xk(2,1)
     c-xk(2,2)*xk(1,3)**2-xk(3,3)*xk(1,2)**2-xk(1,1)*xk(2,3)**2
      ak(1,1)=xk(2,2)*xk(3,3)-xk(2,3)**2
      ak(1,2)=xk(1,3)*xk(2,3)-xk(1,2)*xk(3,3)
      ak(1,3)=xk(1,2)*xk(2,3)-xk(1,3)*xk(2,2)
      ak(2,2)=xk(1,1)*xk(3,3)-xk(1,3)**2
      ak(2,3)=xk(1,2)*xk(1,3)-xk(2,3)*xk(1,1)
      ak(3,3)=xk(1,1)*xk(2,2)-xk(1,2)**2
      ak(2,1)=ak(1,2)
      ak(3,1)=ak(1,3)
      ak(3,2)=ak(2,3)
      return
      end
```